Journal of Medicinal Chemistry

Article

Discovery of a Janus Kinase Inhibitor Bearing a Highly Three-Dimensional Spiro Scaffold: JTE-052 (Delgocitinib) as a New Dermatological Agent to Treat Inflammatory Skin Disorders

Satoru Noji, Yoshinori Hara, Tomoya Miura, Hiroshi Yamanaka, Katsuya Maeda, Akimi Hori, Hiroshi Yamamoto, Shingo Obika, Masafumi Inoue, Yasunori Hase, Takuya Orita, Satoki Doi, Tsuyoshi Adachi, Atsuo Tanimoto, Chika Oki, Yukari Kimoto, Yoshihiro Ogawa, Tamotsu Negoro, Hiromasa Hashimoto, and Makoto Shiozaki

J. Med. Chem., **Just Accepted Manuscript** • DOI: 10.1021/acs.jmedchem.0c00450 • Publication Date (Web): 08 Jun 2020

Just Accepted

is published by the American Chemical Society. 1155 Sixteenth Street N.W., Washington, DC 20036

Discovery of a Janus Kinase Inhibitor Bearing a Highly Three-Dimensional Spiro Scaffold: JTE-052 (Delgocitinib) as a New Dermatological Agent to Treat Inflammatory Skin Disorders

Satoru Noji,[*,†] Yoshinori Hara,[†] Tomoya Miura,[†] Hiroshi Yamanaka,[†] Katsuya Maeda,[†] Akimi Hori,[†] Hiroshi Yamamoto,[†] Shingo Obika,[†] Masafumi Inoue,[†] Yasunori Hase,[†] Takuya Orita,[†] Satoki Doi,[†] Tsuyoshi Adachi,[†] Atsuo Tanimoto,[§] Chika Oki,[§] Yukari Kimoto,[§] Yoshihiro Ogawa,[§] Tamotsu Negoro,[¶] Hiromasa Hashimoto,[†] and Makoto Shiozaki*[*,†]*

[†]Chemical Research Laboratories, [§]Biological Pharmacological Research Laboratories, [¶]Drug Metabolism & Pharmacokinetics Research Laboratories, Central Pharmaceutical Research Institute, Japan Tobacco Inc., 1-1, Murasaki-cho, Takatsuki Osaka, 569-1125, Japan.

KEYWORDS. Janus kinase, SAR, drug-likeness, ligand efficiency, fraction of sp^3, JAK inhibitor, spiro scaffold, JTE-052.

ABSTRACT

Dermatologic disorders such as atopic dermatitis arise from genetic and environmental causes, and are complex and multi-factorial in nature. Among possible risk factors, aberrant immunological reactions are one of the leading etiologies. Immunosuppressive agents including topical steroids are common treatments for these disorders. Despite their reliability in clinical settings, topical steroids display side effects, typified by skin thinning. Accordingly, there is a need for alternate effective and well-tolerated therapies. As part of our efforts to investigate new immunomodulators, we have developed a series of JAK inhibitors, which incorporate novel three-dimensional spiro motifs and unexpectedly possess both excellent physicochemical properties and anti-dermatitis efficacy in the animal models. One of these compounds, JTE-052 (*ent*-**60**), also known as delgocitinib, has been shown to be effective and well-tolerated in human clinical trials, and has recently been approved

in Japan for the treatment of atopic dermatitis as the first drug among Janus kinase inhibitors.

INTRODUCTION

Inflammatory skin disorders are some of the most common forms of dermatological disease. Inflammatory skin disorders are characterized by epidermal hyperplasia along with abnormal keratinocyte differentiation.[1] These disorders encompass a wide range of pathological conditions such as eczema, rosacea, atopic dermatitis (AD), contact dermatitis, pruritus, psoriasis (PS), which afflict roughly 6.1 million patients and impose medical costs of $3 billion annually in the United States alone.[2]

Many of these inflammatory skin disorders are triggered by aberrant immune responses within cells on the surface of the skin, in which cytokine and lymphokine expression is excessively up-regulated.[3,4] Recently, it has become clear that keratinocytes play a critical role in producing those immune mediators, causing them to spread throughout the entire epidermis.[5,6] A primary function of epidermal

keratinocytes is providing a first-line defense against microorganisms and/or other environmental threats; keratinocytes are alerted and activated once diverse stimuli such as pathogens, ultraviolet (UV) light and allergens attack the skin barrier. Despite the diverse and complex etiology of these disorders, topical steroids, which are typically known as immunosuppressive agents, have been used broadly to treat them.[7–9] While the efficacy of topical steroids has been confirmed in the clinic, their side effects, such as skin thinning,[10,11] suggest a need for alternative effective and well-tolerated therapies.

Following the appearance of work by Darnell *et al*,[12] Janus kinase (JAK) inhibition has come to be regarded as a potential pathway for the treatment of certain inflammatory and autoimmune diseases.[13–15] The JAK family of proteins (JAK1, JAK2, JAK3, and Tyk2) possess two kinase domains, a genuine kinase domain and a pseudo-kinase domain having no catalytic activity; hence these proteins are named after the two-faced Roman god Janus. Among the JAK family, critical mutations in JAK3 have been found to lead to severe combined immune deficiency (SCID).[16]

Several research groups have investigated JAK inhibition, including Pfizer.[17–20] In 2006, Pfizer published the results of a Phase II clinical study[21] on the compound

CP-690,550, also known as tofacitinib (**1**) (which was originally reported to be a JAK3 inhibitor, but later was reported to be a pan-JAK inhibitor[18]). In this study, 264 patients with active rheumatoid arthritis (RA) were randomized and subsequently received placebo or three different doses of CP-690,550. CP-690,550 achieved both primary and secondary endpoints in this study, with minor adverse events such as headache and nausea.[21]

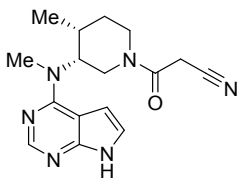

1

Figure 1. Structure of CP-690,550 (tofacitinib).

Structurally, tofacitinib may be regarded as comprising two motifs: a heteroaromatic ring, which adopts a relatively "flat" conformation, and an azacycloalkane group, which, by comparison, displays a relatively greater degree of "three dimensionality". Prior to our work, little had been published about the structure-activity relationships of JAK inhibitors such as tofacitinib. Thus, in our efforts to develop a new series JAK3 inhibitor compounds, we investigated numerous modifications to both these motifs in an attempt to elucidate the SAR of JAK inhibitors.

RESULTS AND DISCUSSIONS

Exploration of the hinge-binding motif

It is currently known that several compounds having ATP-competitive kinase inhibitory activity are typically composed of two units: an adenine mimetic (a so-called "hinge binder") and an accompanying "scaffold" or "head" region. Tofacitinib falls in this category: its pyrrolopyrimidine ring functions as a hinge binder, effecting hydrogen-bonding with the Glu903 and Leu905 residues of the JAK3 protein.[22]

As part of our work, we synthesized and tested multiple compounds with alternative hinge-binding motifs. For these efforts, compound **2** (shown in Table 1) served as our reference compound, and several analogs thereof were synthesized in an attempt to improve upon compound **2**'s JAK3 inhibitory properties. Additionally, to assess the tendency of these compounds to bind off-target, we also measured the inhibitory effects of these compounds against another kinase: lymphocyte-specific protein tyrosine kinase (LCK).[17] Some of these compounds are shown in Table 1 below.

Surprisingly, most of these analogs proved to be largely ineffective against JAK3. From this, we surmise that the binding domain of JAK3 demonstrates a preference for pyrrolopyrimidine. We also note that neither the compounds containing monodentate aromatics (**3** and **4**) nor aliphatic heterocycles (**11**–**13**) show appreciable JAK3 inhibition *in vitro*, and that the inclusion of certain steric or electrostatic features is rarely tolerated (Me, *c*-Pr, and 2-Py for **7**, **8**, and **9**, respectively).

Table1. SAR exploration of the hinge binder starting from compound **2**.[a]

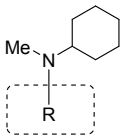

ID	R	IC$_{50}$ (μM)		ID	R	IC$_{50}$ (μM)	
		JAK3[d]	LCK[e]			JAK3[d]	LCK[e]
2	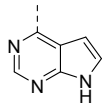	0.079	>10	**9**	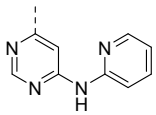	>10	3.3
3	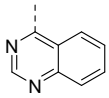	>10	>10	**10**	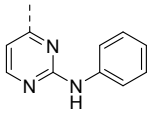	1.8	>10
4[b]	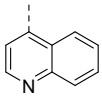	>10	>10	**11**[c]	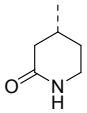	>10	>10
5	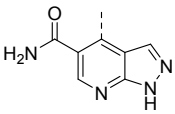	3.0	>10	**12**[b, c]	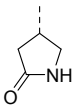	>10	>10
6	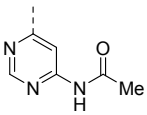	>10	>10	**13**[c]		>10	>10

7	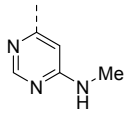	5.0	>10
8	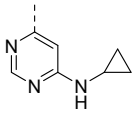	>10	>10

[a]See Experimental Section for assay protocols. The IC_{50} values are the average of at least two determinations. [b]HCl salt form. [c]Racemate. [d]Reference compound **1** gave mean (± SD) IC_{50} = 0.0024 (± 0.00069) μM, *n* = 48. [e]Reference compound **1** gave mean (± SD) IC_{50} = 0.34 (± 0.064) μM, *n* = 36.

Modification of substituents on the hinge binder of compound 10

Based upon our experiments in modifying the hinge binding motif, compound **10**, bearing a phenylamino-pyrimidine substituent in the hinge binding region, was selected for further investigation and modification due to the fact that its JAK3 inhibitory activity and its selectivity for JAK3 over LCK were comparable to those of compound **2**. As further modifications, we investigated a series of hydrophilic substitutions at the para position of the aniline ring (Table 2, R^2).

Several of these compounds achieved JAK3 inhibition at sub-micromolar concentrations, and also inhibited T cell proliferation at similar concentrations (**14**, **16,** and **17**). Compound **15,** however, showed no efficacy against T cell proliferation despite its JAK3 inhibitory activity. We believe that this lack of activity against T cell may be attributable to compound **15**'s poor physical properties (e.g. its low solubility),

a belief that is supported by compound **15**'s inability to inhibit the growth of normal human lung fibroblasts (NHLF)—an assay that we used to measure the off-target toxicity of our compounds against cells other than T cells.

Additional modifications were undertaken at the R^1 position of the pyrimidine ring of compound **10** to explore their potential effects on JAK3 potency and specificity. For these experiments, compound **16** served as our reference compound. Larger substitutions at R^1 generally resulted in decreasing JAK3 potency, with the methyl group showing better JAK3 potency than the ethyl or trifluoromethyl group (**18**–**20**). However, we found the superior LCK selectivity of the trifluoromethyl-bearing compound **20** to be noteworthy.

Table 2. Substitution effects on the hinge binder.[a]

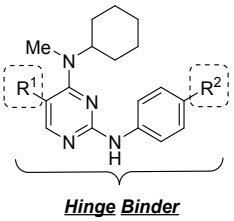

ID	R^1	R^2	IC_{50} (μM)			
			JAK3[b]	LCK[c]	T cell (IL-2)[d]	NHLF[e]
10	H	H	1.8	>10	3.2	>10

14	H	OH	0.41	4.2	0.78	4.6
15	H	O OH	0.073	0.55	>10	>10
16	H	O NH_2	0.11	0.46	0.48	1.1
17	H	O N Me Me	0.21	2.0	0.37	<1.0(65%)
18	Me	O NH_2	0.044	0.34	0.22	2.0
19	Me	O NH_2	0.79	0.40	0.92	3.0
20	F F F	O NH_2	0.077	>10	1.4	2.2

[a]See Experimental Section for assay protocols. The IC_{50} values are the average of at least two determinations. [b]Reference compound **1** gave mean (± SD) IC_{50} = 0.0024 (± 0.00069) μM, *n* = 48. [c]Reference compound **1** gave mean (± SD) IC_{50} = 0.34 (± 0.064) μM, *n* = 36. [d]Reference compound **1** gave mean (± SD) IC_{50} = 0.016 (± 0.087) μM, *n* = 34. [e]Reference compound **1** gave IC_{50} = > 10 μM, *n* = 29.

In an attempt to improve the properties of compound **20** modifications to the "head" region were explored. Specifically, several aliphatic heterocycles were introduced at position R^3. Some of these are shown in Table 3. As shown in Table 3, there was virtually no difference in JAK3 inhibition between compounds **21** and **22**. The effect of substituents on the aliphatic ring were also examined. A 2-methylated analogue (**25**) showed better JAK3 potency than a 3-methylated isomer (**23**). Unfortunately, the selectivity of compound **25** to JAK3 over LCK was significantly

reduced. More disappointingly, a strong cytotoxic effect was observed for compound **25** in NHLF assay, with that compound inhibiting the proliferation of NHLF cells at a concentration of 1 μM. Compound **23**, as well as compound **24** (bearing a 3-hydroxyl substituent) likewise inhibited NHLF growth without any improvement in JAK3 inhibitory activity. In view of these results, we decided to discontinue our further exploration of compounds which, like compound **10**, incorporated a phenylamino-pyrimidine moiety in the hinge binding region.

Table 3. Head motif exploration of **20**.[a]

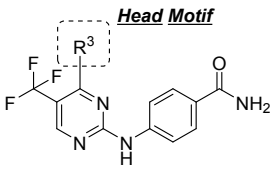

ID	R^3	IC_{50} (μM)			
		JAK3[c]	LCK[d]	T cell (IL-2)[e]	NHLF[f]
21		0.11	>10	2.9	1.3
22		0.12	>10	2.1	1.5
23 *b*	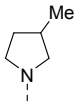	0.061	>10	0.45	1.4
24	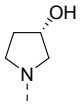	0.053	5.9	1.3	1.8

25[b]		0.018	0.22	0.27	<1.0 (96%)

[a]See Experimental Section for assay protocols. The IC_{50} values are the average of at least two determinations. [b]Racemate. [c]Reference compound **1** gave mean (± SD) IC_{50} = 0.0024 (± 0.00069) μM, *n* = 48. [d]Reference compound **1** gave mean (± SD) IC_{50} = 0.34 (± 0.064) μM, *n* = 36. [e]Reference compound **1** gave mean (± SD) IC_{50} = 0.016 (± 0.0087) μM, *n* = 34. [f]Reference compound **1** gave IC_{50} = > 10μM, *n* = 29.

Exploration of the head motif

In parallel with our investigations of the hinge binding region, we also investigated modifications to the head region, using compound **2** as a reference compound (Table 4). Rather than limit our investigation to relatively "flat" aromatic moieties, a decision was made also to investigate moieties having relatively greater degrees of "three dimensionality". With this consideration in mind, we synthesized and tested numerous compounds, including the three cyclic amines (**30**–**32**) and the other "head" motifs (**26**–**29**) summarized in Table 4. These compounds showed acceptable levels of JAK3 potency and selectivity over LCK. Additionally, we note that the ligand efficiencies (LEs) of compounds **30** and **31** exceed that of compound **2** (0.64, 0.62 vs 0.57). Ligand efficiency (LE) is a theoretical concept that was introduced by Kuntz in 1999[23] and has been characterized as a one potential measure of a

compound's "drug-likeness".[24–26] The LE values of **30** and **31** are superior to those of **26–29**. In view of the promising JAK3, LCK, and LE values for compounds **30** and **31**, we decided to investigate those compounds further.

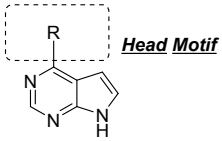

Table 4. SAR of the head motif comprised of pyrroropyrimidine.[a]

ID	R	IC_{50} (μM)			ID	R	IC_{50} (μM)		
		JAK3[d]	LCK[e]	LE[f]			JAK3[d]	LCK[e]	LE[f]
2	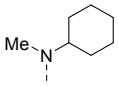	0.079	>10	0.57	**29**[c]		0.33	>10	0.55
26	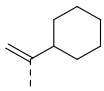	1.1	>10	0.48	**30**		0.26	>10	0.64
27[b, c]	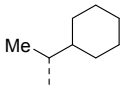	3.7	>10	0.43	**31**		0.16	>10	0.62
28	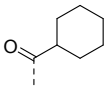	2.7	>10	0.45	**32**		0.42	>10	0.58

[a]See Experimental Section for assay protocols. The IC_{50} values are the average of at least two determinations. [b]Racemate. [c]HCl salt form. [d]Reference compound **1** gave mean (± SD) IC_{50} = 0.0024 (± 0.00069) μM, n = 48. [e]Reference compound **1** gave

mean (± SD) IC_{50} = 0.34 (± 0.064) μM, *n* = 36. [f]LE = −1.37 log IC_{50} (JAK3) / number of heavy atoms.

As shown in Table 5, methyl scanning[27] of compounds **30** and **31** was conducted. 2- or 3-methylation of the cyclic amines led to a slight improvement of JAK3 potency (**33**, **34**, **36**, and **37**), whereas the 4-methylpieridine derivative **35** showed a significant drop in potency. The inclusion of a cyanoacetamide group at the 2- or the 3-position also was examined, with the nitrogen atom therein masked by an additional methyl group (**38** and **39**). Interestingly, compound **38**, bearing a five-membered ring, boosted T cell inhibitory activity whereas compound **39**, bearing a six membered ring, did not show significant T cell inhibitory activity.

In view of these unexpected results, we continued our investigations into the effects that structural changes to cyclic amino head groups might have on T cell inhibitory activity. Our research contrasts with the work of Pfizer, who in 2010 reported that their JAK inhibitor compounds bearing cyclic amino head motifs were less potent than compounds having an *N*-methyl-cycloalkyl head motif.[18]

Compound **40** is an analogue of **38**, with an extra carbon present between the ring and the cyanoacetimide substituent. However, compound **40** exhibited no ability

to inhibit T cell proliferation. These differences in T cell inhibitory activity between **38**–**40** were surprising in view of the general level of structural similarity among these compounds and their comparable JAK3 inhibitory activity.

In an effort to examine the potential effects of conformational freedom vs. conformational constraints within the head region, a series of fused bicyclic compounds was synthesized. Of these, only compound **42** achieved T cell inhibitory activity approaching that of compound **38** while retaining a comparable degree of JAK3 inhibition (IC_{50} = 0.20 μM). The JAK3 potencies of the fused bicyclic compounds **41** and **43** were significantly reduced, with a concomitant loss of T cell potency.

As part of our exploration of conformationally constrained groups, we also synthesized a series of compounds possessing spiro rings. Some of these compounds are shown in Table 5. As demonstrated by compounds **44** and **45**, JAK3 inhibitory activity improved as the size of the terminal ring became larger, though these improvements did not necessarily translate to improved T cell inhibitory activities. Additionally, reduced *in vitro* potencies were observed for compound **46**, in which the cyanoacetyl moiety is located at the gamma position toward the nitrogen atom of the inner pyrrolidine ring; these reduced potencies for compound **46** suggested that the

relative position of the cyanoacetyl moiety within the head region could have important effects on activity. Collectively, these results suggested to us that there might be some appropriate combination of ring sizes within a spiro group that might achieve acceptable levels of JAK3 inhibition. In view of those results, we conducted further experiments on compounds that included a piperidine ring as part of the spiro group, while varying the size of the terminal ring. Some of these spiro compounds are shown in Table 5. Among compounds **47–49**, compound **47** exhibited the best inhibitory activity against both JAK3 and T cell proliferation.

Table 5. SAR of the head motif focused on cyclic amines.[a]

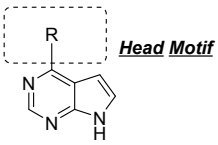

ID	R	IC$_{50}$ (μM)				Fsp^{3}[f]
		JAK3[b]	LCK[c]	T cell (IL-2)[d]	NHLF[e]	
33	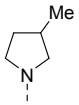	0.094	>10	3.0	>10	0.46
34		0.082	>10	3.5	>10	0.46
35	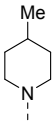	>1.0	5.5	>10	>10	0.50

36	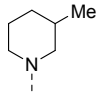	0.13	>10	2.4	>10	0.50
37	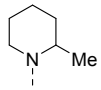	0.14	>10	2.4	>10	0.50
38	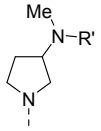	0.40	>10	0.15	>10	0.43
39	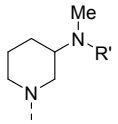	0.30	>10	1.7	>10	0.50
40	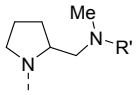	0.66	>10	>10	>10	0.47
41	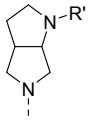	1.2	>10	>10	>10	0.47
42	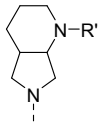	0.20	>10	0.22	>10	0.50
43	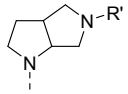	2.7	>10	>10	>10	0.47
44	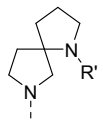	0.088	>10	0.15	>10	0.50
45	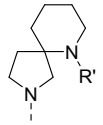	0.048	4.1	0.25	3.9	0.53
46	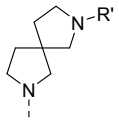	0.64	>10	1.8	>10	0.50
47	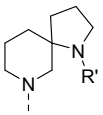	0.036	6.3	0.048	>10	0.53
48	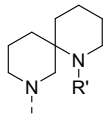	0.041	0.63	0.086	3.9	0.56

49	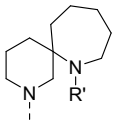	0.18	5.0	2.2	3.4	0.58

[a]All compounds are racemates. R' = cyanoacetyl. See Experimental Section for assay protocols. The IC_{50} values are the average of at least two determinations. [b]Reference compound **1** gave mean (± SD) IC_{50} = 0.0024 (± 0.00069) μM, *n* = 48. [c]Reference compound **1** gave mean (± SD) IC_{50} = 0.34 (± 0.064) μM, *n* = 36. [d]Reference compound **1** gave mean (± SD) IC_{50} = 0.016 (± 0.0087) μM, *n* = 34. [e]Reference compound **1** gave IC_{50} = > 10 μM, *n* = 29. [f]Fsp^3 = number of sp^3 hybridized carbons/total carbon count.[28]

In an attempt to improve upon the activity of compound **47**, we adopted a two-pronged approach, on the one hand synthesizing compounds incorporating other spiro rings, and on the other hand investigating other acyl substituents. Our efforts to synthesize other spiro rings created significant synthetic challenges for our chemists. Specifically, the literature at the time was devoid of reliable methods for making a diazaspirocycle incorporating an azetidine ring. We therefore had to develop a reliable method by ourselves, for which our extensive efforts are described later in this publication. In the meantime, our investigations into other acyl substituents yielded results such as those shown in Table 6. Compounds **50**–**53** showed reduced cell potency compared to the cyanoacetyl substituent of compound **47**.

Table 6. SAR of the acyl group on the head group.[a]

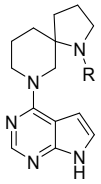

ID	R	IC$_{50}$ (μM)			
		JAK3[b]	LCK[c]	T cell (IL-2)[d]	NHLF[e]
47	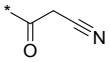	0.036	6.3	0.048	>10
50		0.25	>10	N.T[f]	N.T[f]
51	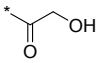	0.067	5.8	0.19	>10
52	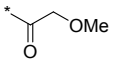	0.17	>10	N.T.[f]	N.T.[f]
53	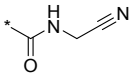	0.010	4.5	0.22	>10

[a]All compounds are racemates. See Experimental Section for assay protocols. The IC$_{50}$ values are the average of at least two determinations. [b]Reference compound **1** gave mean (± SD) IC$_{50}$ = 0.0024 (± 0.00069) μM, n = 48. [c]Reference compound **1** gave mean (± SD) IC$_{50}$ = 0.34 (± 0.064) μM, n = 36. [d]Reference compound **1** gave mean (± SD) IC$_{50}$ = 0.016 (± 0.0087) μM, n = 34. [e]Reference compound **1** gave IC$_{50}$ = > 10 μM, n = 29. [f]Not tested.

Investigation of diazaspiroalkane-based JAK inhibitors

Compound **54** was synthesized according to a newly-developed method. This compound, incorporating an azetidine ring as part of its spiro group, demonstrated good T cell inhibitory activity (Table 7). Encouraged by this result, we made further

modifications to this compound. The results are included in Table 7. Among four methylated analogs (**55**–**58**), compound **57**, bearing a methyl adjacent to the quaternary carbon, displayed improved JAK3 potency. The *gem*-dimethyl analogue **58** displayed comparatively less JAK3 potency, though its difluoro analogue **59** achieved JAK3 and T cell results comparable to those of **57**. Compound **60** and **61**, pyrrolidine analogs of **57** and **59**, respectively, displayed activity against T cell proliferation roughly comparable to that of compounds **57** and **59**.

Table 7. SAR of azetidine-associated diazaspirocycle derivatives.[a]

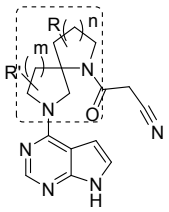

ID	Structure	IC$_{50}$ (μM)				Fsp^{3}[h]
		JAK3[d]	LCK[e]	T cell (IL-2)[f]	NHLF[g]	
54	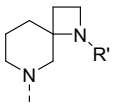	0.038	3.7	0.051	>10	0.50
55[b]	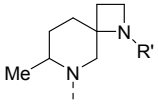	0.41	8.6	N.T.[i]	N.T.[i]	0.53
56[b]	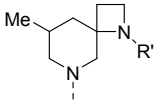	0.058	5.2	0.10	>10	0.53

57[b, c]	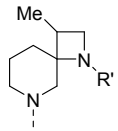	0.0070	1.5	0.032	>10	0.53
58	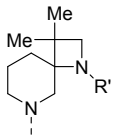	0.13	>10	2.0	>10	0.56
59	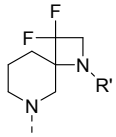	0.0064	2.6	0.048	>10	0.48
60[b, c]	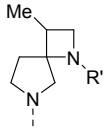	0.021	>10	0.039	>10	0.50
61	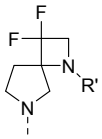	0.011	4.7	0.055	>10	0.47

[a]All compounds are racemates. R' = cyanoacetyl. See Experimental Section for assay protocols. The IC_{50} values are the average of at least two determinations. [b]Single diastereomer (the absolute stereochemistry was not defined.) [c]Both of the diastereomers were obtained. Data for the more potent compound in terms of JAK3 inhibitory activity is shown. [d]Reference compound **1** gave mean (± SD) IC_{50} = 0.0024 (± 0.00069) μM, n = 48. [e]Reference compound **1** gave mean (± SD) IC_{50} = 0.34 (± 0.064) μM, n = 36. [f]Reference compound **1** gave mean (± SD) IC_{50} = 0.016 (± 0.0087) μM, n = 34. [g]Reference compound **1** gave IC_{50} > 10 μM, n = 29. [h]Fsp^3 = number of sp^3 hybridized carbons/total carbon count.[28] [i]Not tested.

The spiro-based compounds listed in Table 8 were isolated in enantiomerically pure form and characterized in pharmacokinetic assays. Although these compounds displayed comparable IC_{50} values in *in vitro* JAK3 inhibitory and T cell proliferation

assays, meaningful differences appeared among them in assessing their pharmacokinetic profiles.

Generally, compounds incorporating a piperidine ring (*ent*-47–*ent*-59) were discovered to be more readily metabolized, while the pyrrolidine analogues, *ent*-60 and *ent*-61, were metabolically more stable across the tested species.

Among the two pyrrolidine analogs, *ent*-60 exhibited both greater potency against T cells and a lower clearance rate in monkeys than *ent*-61, thereby suggesting that *ent*-60 might be more potent and display longer-lasting effects in an *in vivo* setting. Additionally, it was decided that the synthesis of *ent*-61 imposed cost ineffectiveness that could be avoided with *ent*-60. Accordingly, *ent*-60 was selected as a candidate for clinical development, and was renamed JTE-052.

Table 8. Representative JAK inhibitors possessing a spirodiazacycloalkane.[a]

ID	IC_{50} (μM)		MS (%, 60min)		CL monkey[d]
	JAK3[b]	T cell (IL-2)[c]	human	monkey	(L/hr/kg)
ent-47	0.011	0.041	75.7	29.4	N.T.[e]
ent-54	0.019	0.017	93.4	85.2	0.76
ent-57	0.0040	0.011	73.4	25.1	N.T.[e]
ent-59	0.0060	0.019	88.4	64.6	N.T.[e]

ent-60	0.013	0.0089	97.4	99.6	0.29
ent-61	0.011	0.033	99.4	95.4	0.35

[a]See Experimental Section for assay protocols. The IC_{50} values are the average of at least two determinations. [b]Reference compound **1** gave mean (± SD) IC_{50} = 0.0024 (± 0.00069) μM, n = 48. [c]Reference compound **1** gave mean (± SD) IC_{50} = 0.016 (± 0.0087) μM, n = 34. [d]Administered intravenously at 0.1 mg/kg. [e]Not tested.

In order to clarify the mechanism of high potency of JTE-052 against JAK3, X-ray co-crystal analysis was performed with compound **60**. Only one of the enantiomers gave a good crystal with a high resolution of 1.98 Å, suggesting that this enantiomer (*ent*-**60**) was an active isomer (Figure 2).[29] According to the structure, the cyanoacetyl group made orthogonal dipolar interactions with main chain atoms (Gly829–Lys830 and Gly834–Ser835), while the azetidine motif occupied the lipophilic pocket neighborhood the JAK3 hinge region with the 7*H*-pyrrolo[2,3-*d*]pyrimidine ring making hydrogen bond interactions with JAK3 hinge region of Glu903 (2.6 Å) and Leu905 (2.9 Å). It was thus presumed that the potent JAK3 activity of JTE-052 was attributed to those interactions.

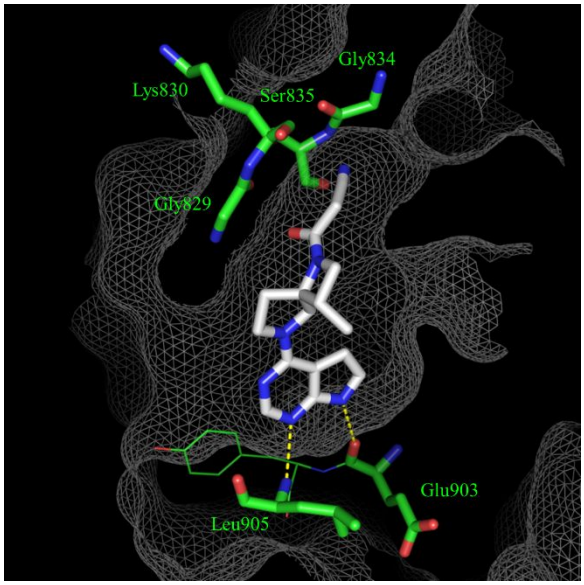

Figure 2. X-ray crystallographic structure of JAK3 (human) in complex with JTE-052 focusing on binding site (PDB code 7C3N). Hydrogen bonds are depicted as dashed lines (yellow). Surface are showed around JTE-052 as meshed lines.

As a part of our further characterizations, the selectivity of JTE-052 for JAK3 was investigated in comparison with the other members of the JAK family and a panel of 50 other human kinases. As shown in Table 9, JTE-052 was found to exhibit inhibitory activity across all JAK family members (JAK3, JAK1, JAK2 and Tyk2) and inhibited JAK1 and JAK2 at nanomolar concentrations. As can be seen from the data in Table 9, the inhibitory activity of JTE-052 across the JAK family differs from that of tofacitinib; interestingly, JTE-052 exhibits relatively greater inhibitory activity against JAK1 and JAK2 than JAK3 compared to tofacitinib, and its selectivity for the JAK family over LCK is improved in comparison with tofacitinib. JTE-052 also proved to be highly selective for the JAK family members, with no significant inhibition of non-JAK kinases under 1 μM

except over ROCK-II.[30] Surprisingly, the potency of JTE-052 in whole-cell assays is not linearly correlated with its potency against JAK kinases, as was sometimes observed in other kinase inhibitor programs.[31] For example, we expected that the IC_{50} values of JTE-052 against IL-6/GM-CSF signaling would be correlated with JTE-052's activity against each JAK isozyme. However, the results in Table 9 below show that JTE-052 suppressed JAK1-dependent signaling at an IC_{50} value tenfold below the IC_{50} value required to suppress JAK2-dependent signaling (IL-31/GM-CSF). The exact mechanism of such discrepancy between the enzymatic inhibition and the cell potency is not fully understood; it seemed that potency against JAK1 enzyme predominantly accounted for the results of cytokine signaling inhibitions. This suggestion is supported, for example, by the reported K_m value for JAK1, which is about ten times that of JAK3, making JAK1 easier to inhibit than JAK3 at the same ATP concentration.[32,33] Consequently, it is likely that much of the efficacy observed in the *in vivo* models is driven by JAK1. Regardless, JTE-052's effective suppression of IL-2 and IL-31 signaling pathways further bolstered its potential as a clinical candidate.

Table 9. *In vitro* profiles of JTE-052.[a]

ID	Enzymes IC_{50} (μM)				
	JAK3	JAK1	JAK2	TyK2	LCK
JTE-052	0.013	0.0028	0.0026	0.058	5.8
Tofacitinib	0.0011	0.0029	0.0012	0.042	0.44

ID	Cytokine signaling IC_{50} (μM) in human PBMCs					
	IL-2[b] JAK1/JAK3	IL-6[c] JAK1/JAK2	IL-31[d] JAK1/JAK2	IL-23[e] JAK2/Tyk2	GM-CSF[f] JAK2/JAK2	INF-α[g] JAK1/Tyk2
JTE-052	0.040	0.033	0.025	0.084	0.30	0.018

[a]The IC_{50} values are the average of at least two determinations. [b]The phosphorylation levels of Stat5 in $CD3^+CD4^+$ cells stimulated with IL-2 were measured. [c]The phosphorylation levels of Stat3 in $CD3^-CD4^+$ cells stimulated with IL-6 were measured. [d]The phosphorylation levels of Stat3 in A549 cells stimulated with IL31 were measured. [e]The phosphorylation levels of Stat3 in $CD3^+CD4^+$cells stimulated with IL-23 were measured. [f]The phosphorylation levels of Stat5 in $CD3^-CD4^+$ cells stimulated with GM-CSF were measured. [g]The phosphorylation levels of Stat1 in $CD3^+CD4^+$ cells stimulated with INF-α were measured.

Pharmacokinetic properties of JTE-052 were characterized (Table 10). In these tests, the solubility of JTE-052 proved acceptable in several media, and protein binding was low in the tested species.

Table 10. Physicochemical properties and PK profiles of JTE-052.

LogD (pH 7)	Caco2		Solubility (μM)			Protein Binding (%)			
	Pap $10cm^{-8}$	Sol μM	PBS	Fassif	Fessif	human	rat	dog	monkey

0.6	3.3	1.0	>95	>475	>475	40.7	37.2	27.1	26.6

JTE-052 was also metabolically stable in both liver microsomes and hepatocytes, with stability values in human cells greater than those in rat and monkey cells (Table 11). The *in vivo* PK profiles of JTE-052 were also satisfactory showing over 50% of bioavailability across the species (Table 12).

Table 11. Metabolic stability of JTE-052.

	Metabolized stability (60min, %)			
	human	rat	dog	monkey
Microsome	97.4	90.2	97.2	99.6
Hepatocyte	99.3	94.7	N.T.[a]	84.8

[a]Not tested.

Table 12. *In vivo* PK profiles of JTE-052.

	iv PK parameters[a]					po PK parameters[b]			
	dose	t1/2β	Cltot	Vdss	MRT	dose	tmax	Cmax	F
speci	(mg/kg	(h)	(L/h/kg)	(L/kg)	(h)	(mg/kg	(h)	(ng/mL)	(%)
rat	1.0	1.7	2.1	2.1	1.0	10	1.5	2.5	78
dog	0.3	2.3	0.37	1.2	3.2	1.0	0.9	1.9	124

[a]iv administration at corresponding dose in 10% DMSO. [b]po administraion at corresponding dose in 0.5% MC.

To explore the *in vivo* pharmacological effects of JTE-052, a rat adjuvant-induced arthritis (AIA) model was chosen based on the robustness and the reproducibility of this animal model.[34,35] As shown in Figure 3a, dose-dependent suppression of paw swelling was observed; complete suppression of paw swelling was observed at a dose of 30 mg/kg of JTE-052 upon oral administration. The anti-dermatitis effects of JTE-052 were confirmed in a rat 2,4-dinitrochlorobenzene (DNCB)-induced dermatitis model[36,37], in this model, complete suppression of ear swelling was achieved at an oral dose of 10 mg/kg (Figure 3b). Additionally, topical formulations of JTE-052 for AD treatment were examined in the rat DNCB model (Figure 3c). Treatment using 1% JTE-052 in a petroleum-based ointment produced significant suppression of ear swelling; three-times-a-day administration of the JTE-052 ointment almost completely suppressed ear swelling in this model.

(a)

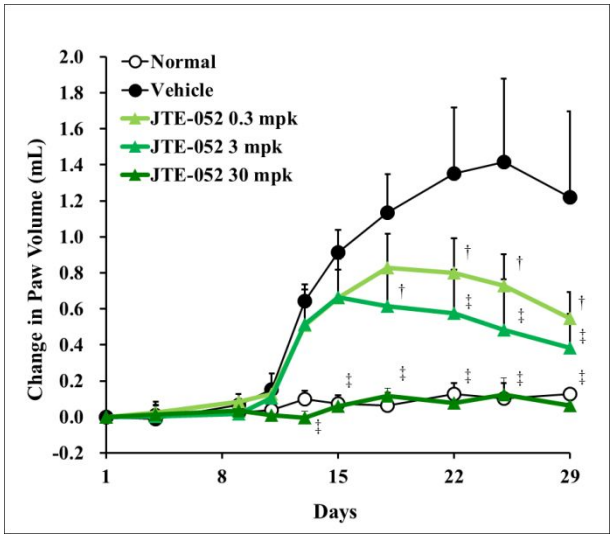
Normal
Vehicle
JTE-052 0.3 mpk
JTE-052 3 mpk
JTE-052 30 mpk
Change in Paw Volume (mL)
Days

(b)

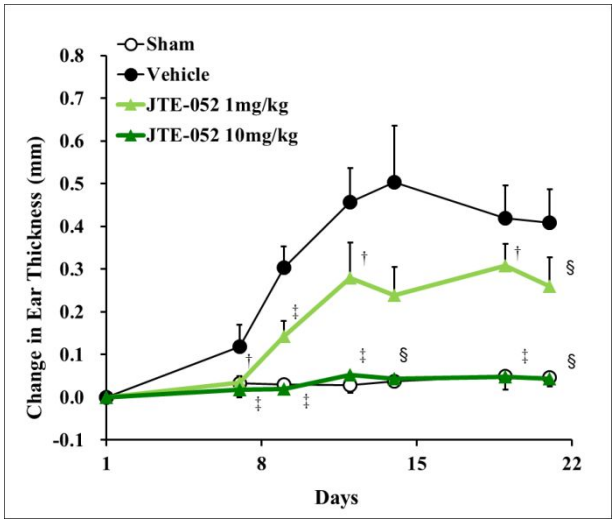
Sham
Vehicle
JTE-052 1mg/kg
JTE-052 10mg/kg
Change in Ear Thickness (mm)
Days

(c)

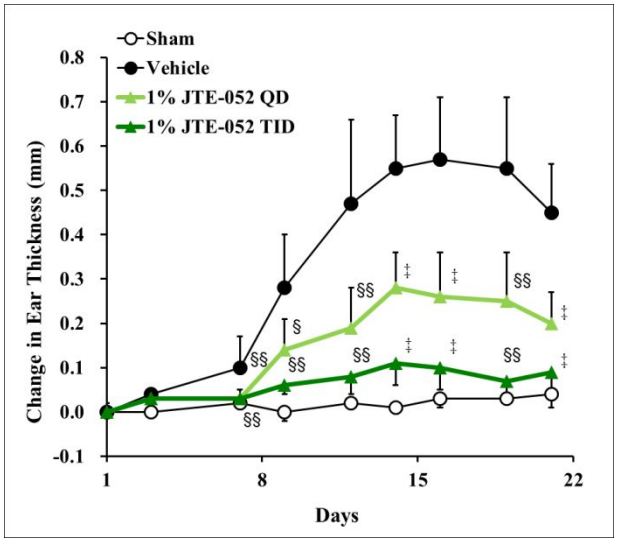

Figure 3. *In vivo* potency of JTE-052. (a) Effect of JTE-052 at 30, 3, and 0.3 mg/kg by po administration on the hind paw volume in a rat adjuvant-induced arthritis (AIA) model. The results are expressed as mean ± SD (n = 4). †, ‡ : $p<0.05$, $p<0.01$ vs. vehicle group by Dunnett's test. (b) Effect of JTE-052 at 10 and 1 mg/kg by po administration on the ear thickness in a rat DNCB-induced chronic dermatitis model. The results are expressed as mean ± SD (n = 3–4). †, ‡ : $p<0.05$, $p<0.01$ vs. vehicle group by Dunnett's test. § : $p<0.05$ vs. vehicle group by Steel test. (c) Effect of JTE-052 ointment at once a daily and three times a day on the ear thickness in a rat DNCB-induced chronic dermatitis model. The results are expressed as mean ± SD (n = 3–4). ‡ : $p<0.01$ vs. vehicle group by Dunnett's test. §, §§: $p<0.05$, $p<0.01$ vs. vehicle group by Steel test.

Chemistry

Synthesis of JAK inhibitors listed in Table 1

Synthetic pathways of JAK inhibitors listed in Table 1 are categorized into two groups depending on the key reactions, *N*-arylation and reductive amination, respectively (Scheme 1). Regarding the *N*-arylation-centered pathway, an aryl

chloride was firstly coupled with *N*-methylcyclohexylamine at elevated temperature with or without a metal catalysis, followed by simple transformations to give **3–10**. Meanwhile, **11–13** were synthesized via reductive amination, in which cyclohexylmethyl amine or an aminolactam was treated with an appropriate ketone in the presence of $NaBH(OAc)_3$.

Scheme 1. Synthesis of JAK inhibitors composed of various hinge binders (**3–13**).[a]

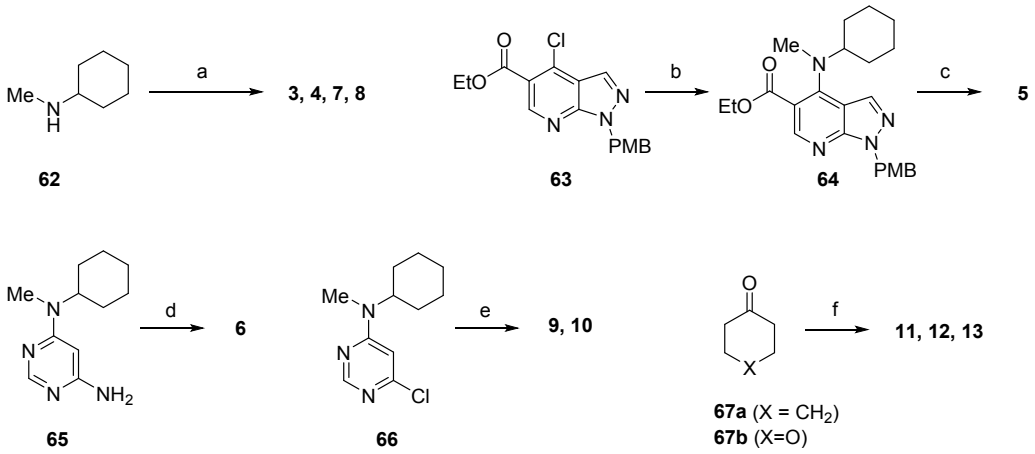

[a]Reagents and conditions: (a) for **3**, 4-chloroquinazoline, *i*-Pr_2NEt, THF, microwave, 80 °C; for **4**, (i) 4-chloroquinoline, $Pd_2(dba)_3$, DAVEPHOS, NaO*t*-Bu, 1,4-dioxane, 80 °C; (ii) 4 N HCl in EtOAc; for **7** and **8**, corresponding heteroaryl chloride, *n*-BuOH, 145 °C; (b) *N*-methylcyclohexylamine, EtOH, 80 °C; (c) (i)TFA, anisole, 70 °C; (ii) 4 N NaOH, EtOH, 120 °C; (iii) $SOCl_2$, toluene, 60 °C, (iv) 28% NH_3 aq., THF, rt; (d) (i) AcCl, Et_3N, DMAP, $CHCl_3$, 0 °C, (ii) $LiOH{\cdot}H_2O$, THF, MeOH, H_2O; (e) for **9**, 2-aminopyridine, $Pd(OAc)_2$, DPEphos, K_2CO_3, THF, 80 °C; for **10**, ethyl 4-aminobenzoate, $Pd(OAc)_2$, DPEphos, K_2CO_3, THF, 80 °C; (f) (i) for **11** and **12**, corresponding amino lactam, $NaBH(OAc)_3$, AcOH, $CHCl_3$, rt; (ii) HCHO, $NaBH(OAc)_3$, AcOH, $CHCl_3$, rt; for **13**, (i) *N*-

methylcyclohexylamine, TsOH, toluene, 90 °C then $NaBH_4$, EtOH, rt; (ii) 4 N HCl in EtOAc, rt.

Synthesis of JAK inhibitors listed in Table 2 and 3

Compounds listed in Table 2 were synthesized through the *N*-arylation-centered protocol as well (Scheme 2). Starting from compound **68**, 4-aminobenzoate was coupled in the presence of Pd catalyst, and the ester substituent on the benzene ring was further derivatized to the corresponding alcohol (**14**), carboxylic acid (**15**) and amide functionalities (**16**–**20**). Compound **21**–**25** were synthesized similarly, although compound **72** was chosen as the common intermediate to be coupled with cyclic amino motifs in the final step (Scheme 3).

Scheme 2. Synthesis of JAK inhibitors listed in Table 2 (**14**–**20**).[a]

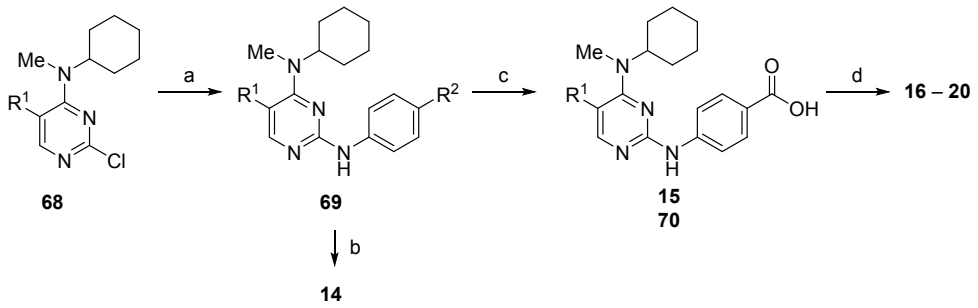

[a]Reagents and conditions: (a) methyl 4-aminobenzoate, $Pd(OAc)_2$, DPEphos, K_2CO_3, THF, 80 °C; (b) $LiAlH_4$, THF, rt; (c) $LiOH{\cdot}H_2O$, THF, MeOH, H_2O, 50 °C; (d) NH_4Cl or $NHMe_2$, *i*-Pr_2NEt, WSC·HCl, HOBt·H_2O, DMF, rt.

Scheme 3. Synthesis of biaryl amine-based JAK inhibitors listed in Table 3 (**21**–**25**).[a]

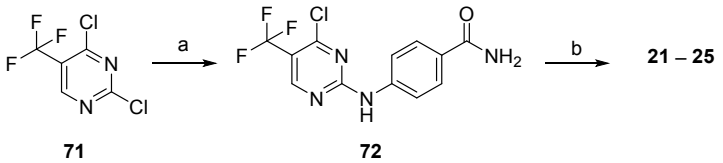

[a]Reagents and conditions: (a) 4-aminobenzamide, *i*-Pr_2NEt, THF, rt; (b) corresponding amine, *i*-Pr_2NEt, DMA, 80°C.

Synthesis of analogues of compound 2

Synthesis of compound **26**–**29**, analogues of compound **2** were illustrated in Scheme 4. Suzuki-type cross-coupling of **73** with vinyl borane afforded **26** which was successively derivatized to **27** via hydrogenation reaction. Coupling of **73** with cyclohexanol also proceeded smoothly and *O*-arylated product **29** was obtained under the mild condition. Halogen-metal exchange was carried out by treatment of **74** with *i*-PrMgCl, and the resultant aryl Grignard reagent was coupled with cyclohexyl chloride, leading to compound **28** after deprotection of the tosyl group

Scheme 4. Synthesis of JAK inhibitors bearing a pyrrolopyrimidine (**26–29**).[a]

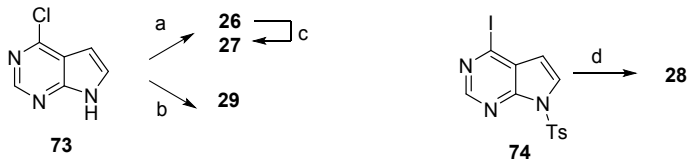

[a]Reagents and conditions: (a) 2-(1-cyclohexylvinyl)-4,4,5,5-tetramethyl-1,3,2-dioxaborolane, $Pd(PPh_3)_4$, 2 N Na_2CO_3, DME, microwave, 150°C; (b) (i) cyclohexanol, NaH, THF, 80 °C; (ii) 4 N HCl in EtOAc, rt; (c) (i) H_2 (1 atm), Pd/C, EtOAc, rt; (ii) 4 N HCl in EtOAc, rt; (d) (i) cyclohexanecarbonyl chloride, *i*-PrMgCl, bis[2-*N*,*N*-dimethylaminoethyl]ether, THF, 0 °C; (ii) 2 N NaOH, THF, MeOH, rt.

Synthesis of JAK inhibitors possessing an azacycloalkane head motif

Generally, JAK inhibitors bearing an azacycloalkane head group were synthesized by *N*-arylation of **73** with the assistance of microwave heating, which was followed by deprotection and successive cyanoacetylation when needed (Scheme 5).

Scheme 5. Synthesis of JAK inhibitors bearing a pyrrolopyrimidine (**30–53**).[a]

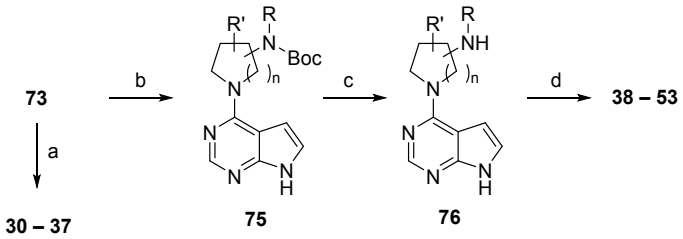

[a]Reagents and conditions: (a) corresponding cyclic amine, *t*-BuOH, microwave, 100 °C; (b) correponding cyclic amime, K_2CO_3, H_2O, 100 °C; (c) 4 N HCl in EtOAc rt; (d) for **38–49**, 3-(3,5-dimethyl-1*H*-pyrazol-1-yl)-3-oxopropanenitrile, *i*-Pr_2NEt, 1,4-dioxane, 80 °C; for **50**, AcCl, Et_3N, $CHCl_3$, 0 °C; for **51**, (i) acetoxyacetyl chloride,

Et_3N, $CHCl_3$, 0 °C; (ii) K_2CO_3, MeOH, rt; for **52**, 2-methoxyacetyl chloride, Et_3N, $CHCl_3$, 0 °C; for **53**, 4-nitrophenyl (cyanomethyl)carbamate, *i*-Pr_2NEt, DMA, rt.

Synthetic exploration for an azetidine-associated diazaspiroalkane

Synthetic strategies to obtain novel diazaspirocycle motifs are depicted in Figure 4. Path A was firstly investigated starting from an azetidine carboxylate.

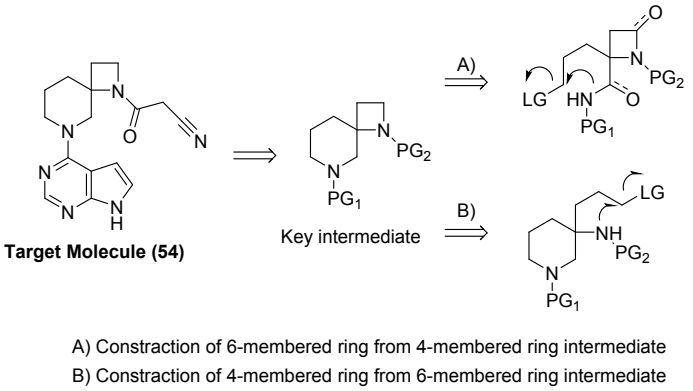

Figure 4. Synthetic strategy for a diazaspiroalkane containing an azetidine ring.

After Boc protection of commercially available compound **77**, the carboxylic acid was converted to the cyano group (**80**), followed by its α-alkylation to give **81**. Subsequent Raney-Nickel reduction was hoped to afford the desired product via self-cyclization; however, the reaction did not work, and only a complex mixture was obtained (Scheme 6).

Scheme 6. Route scouting based on path A from compound **77**.[a]

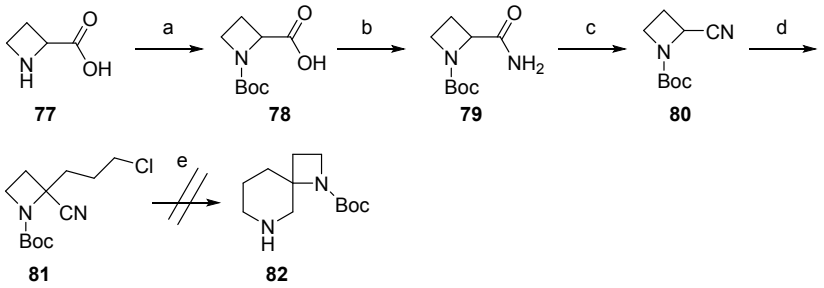

[a]Reagents and conditions: (a) $(Boc)_2O$, 0.5 N NaOH, 1,4-dioxane, 0°C to rt (62%); (b) CDI, NH_4Cl, Et_3N, THF, 0°C to rt (quant); (c) TFAA, Et_3N, CH_2Cl_2, 0°C to rt (45%); (d) KHMDS, 1-bromo-3-chloropropane, THF, −78 °C to rt (17%); (e) H_2 (4 atm), Raney Ni, 28% NH_3aq. MeOH, rt.

Since the chloroalkyl moiety seemed to be labile and may have been the possible cause for complications, a more conservative approach was next examined (Scheme 7). Cbz-protected azetidine carboxylate **83** was treated with allyl bromide in the presence of K_2CO_3, and the resultant ester was subjected to Claisen rearrangement to translocate the allyl substituent on the azetidine ring. Although optimal conditions were not fully explored, pathways involving hydroboration of compound **84** were explored. Unfortunately, several trials attempting to produce the targeted dialkylamine (**88**) either by way of *N*-alkylation or reductive amination was not

successful, which brought us to Path B, using a piperidine-based compound as a starter.

Scheme 7. Route scouting based on path A from compound **83**.[a]

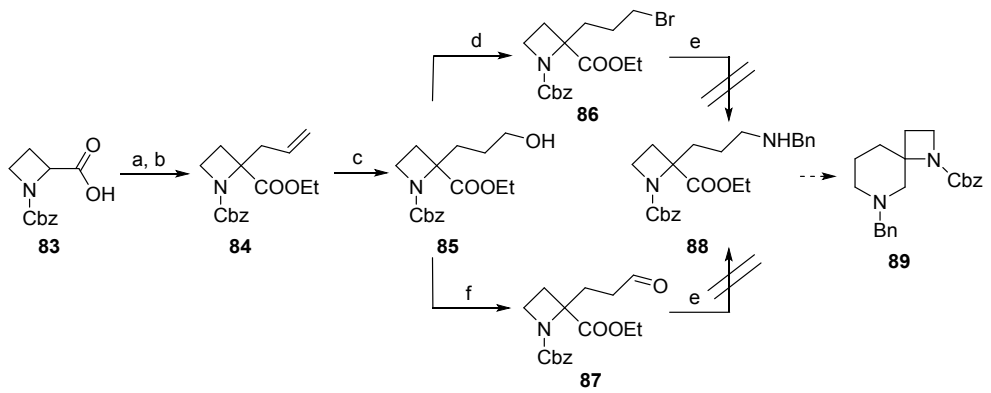

[a]Reagents and conditions: (a) K_2CO_3, EtI, DMF, rt, (97%) (b) LiHMDS, allyl bromide, THF, −78°C (88%); (c) BH_3, THF, rt then 4 N NaOH, H_2O_2, 0°C, (29%); (d) CBr_4, PPh_3, CH_2Cl_2, rt (62%); (e) $BnNH_2$, K_2CO_3, DMF, 120 °C (trace); (f) DMP CH_2Cl_2, rt (75%).

Initially, [2+2]-cyclization was attempted with compound **91**, which was easily obtained from commercially available **90**. The result was also disappointing and no sign of spiro ring formation was observed (Scheme 8).

Scheme 8. Route scouting based on path B from compound **90**.[a]

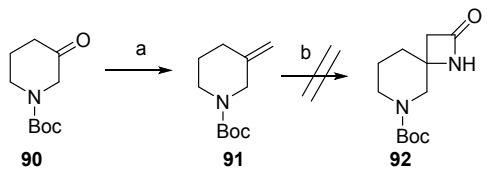

[a]Reagents and conditions: (a) $Ph_3P^+MeBr^-$, KO*t*-Bu, THF, rt, (85%); (b) $ClSO_2NCO$, Et_2O, rt.

A Horner-Wadsworth-Emmons reaction with **90** followed by 1,4-addition of methanolic ammonia successfully provided every necessary unit for constructing the desired spirocycle (**99**). After ester hydrolysis, the resultant amino acid **95** was treated with tris(2-oxo-3-benzoxazolinnyl phosphine oxide[38] and Et_3N to form the targeted spirocyclic skeleton (**96**). After protecting the amide NH with benzyl group (**97**), Boc deprotection and subsequent LAH reduction finally achieved to affording compound **99**. Followed by coupling with pyrrolopyrimidine, deprotection, and cyanoacetylation, our targeted compound **54** was successfully obtained (Scheme 9).

Scheme 9. Synthesis of JAK inhibitor bearing a spirocycle (**54**).[a]

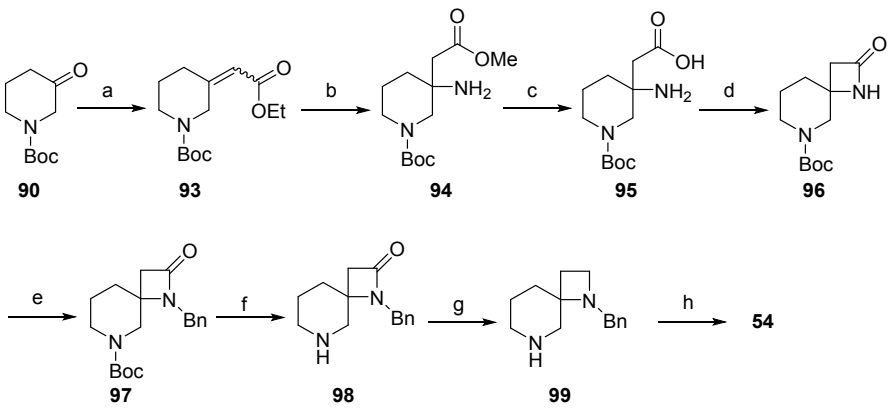

[a]Reagents and conditions:(a) $(EtO)_2POCH_2CO_2Et$, NaH, THF, 0 °C to rt; (b) NH_3 in MeOH, 80 °C; (c) 2 N NaOH, MeOH, rt; (d) tris(2-oxo-3-benzoxazolinnyl phosphine oxide, Et_3N, CH_3CN, 100°C; (e) BnBr, NaH, DMF, rt; (f) 4 N HCl in EtOAc, rt then sat.$NaHCO_3$; (g) $LiAlH_4$, H_2SO_4, THF, 0 °C; (h) (i) **73**, K_2CO_3, H_2O, 100 °C; (ii) Pd/C, H_2 (4 atm), MeOH, rt.; (iii) 3-(3,5-dimethyl-1*H*-pyrazol-1-yl)-3-oxopropanenitrile, *i*-Pr_2NEt, 1,4-dioxane, 100 °C.

Additionally, an alternative synthetic approach to cover broader range of diazaspiroalkanes was explored (Scheme 10). Starting from the 3-pyrrolidine or 3-piperidine carboxylic acid **100**, allyl ester formation (**101**) followed by Claisen rearrangement gave the α-allylated carboxylate **102,** which was subjected to a Curtius rearrangement reaction. The reaction proceeded smoothly and **103** was converted to **104** by way of ozonolysis and subsequent reduction. Cbz group of **104** was thus removed by hydrogenolysis and the resultant β-amino alcohol was derivatized to the aminoethyl bromide, which automatically formed the azetidine ring. After re-protecting the nitrogen atom with Cbz group (**105**), Boc protetion was removed to give **106** which

was advanced to **55–61** according to the general synthetic method described before in this report (Table 7).

Scheme 10. Synthesis of JAK inhibitors bearing various spirocycles (**55–61**).[a]

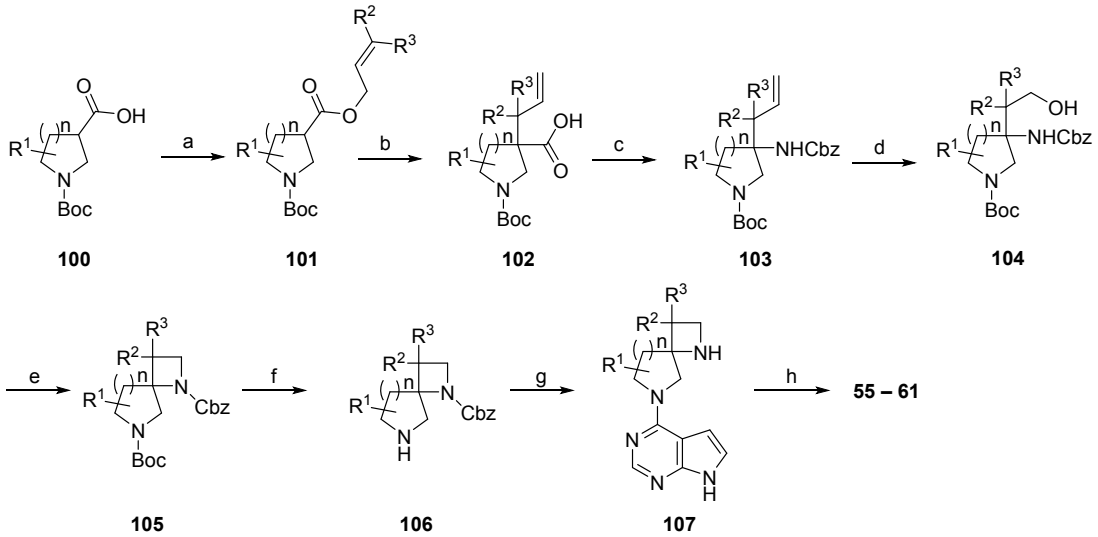

[a]Reagents and conditions: (a) $BrCH_2CH{=}CR^2R^3$, K_2CO_3, DMF, rt; (b) LiHMDS, THF, −78 °C to rt then TMSCl, −78 °C to rt; (c) (i) DPPA, Et_3N, toluene, 100 °C, then BnOH, DMAP, 100 °C; (d) O_3, $CHCl_3$, MeOH, −78 °C then $NaBH_4$, −78 °C to rt; (e) (i) H_2 (1atm), Pd/C, THF, rt; (ii) Et_3N, Ph_3P, CBr_4, CH_2Cl_2, 0 °C; (iii) *i*-Pr_2NEt, CbzCl, 0 °C; (f) 4 N HCl in 1,4-dioxane, $CHCl_3$, rt; (g) (i) **73**, K_2CO_3, H_2O, 100 °C; (ii) Pd/C, H_2 (4 atm), THF, MeOH, rt; (h) 3-(3,5-dimethyl-1*H*-pyrazol-1-yl)-3-oxopropanenitrile, *i*-Pr_2NEt, 1,4-dioxane, 80 °C.

Stereoselective synthesis of JTE-052

In order to develop a stereoselective synthetic route for JTE-052, (*S*)-benzylalaninol was selected as a starting material whose inherent chirality dictated the

stereochemistry of the final product. Firstly, *N*-alkylation of this starting material with *t*-butyl bromoacetate was carried out, and the concomitant alcohol (**109**) was successively chlorinated, resulting in intramolecular *N*-alkylation to form a highly reactive aziridinium ring (**111**). Upon heating, an accompanying chloride anion attached to the constrained ring and compound **112** was eventually obtained due to its thermodynamic stability over the corresponding regioisomer. This compound was then treated with LHMDS at −78 °C and intramolecular cyclization proceeded in a S_N2 fashion to give **113** as a single enantiomer.[39] After modifying protecting groups, α-alkylation of the carboxylate (**114**) with sterically-demanding prenyl bromide was carried out and the reaction underwent anti to the methyl substituent, so that the carbon skeleton of the spirocycle motif was obtained with high enantiomeric selectivity. To introduce a nitrogen atom for the pyrroridine motif, **115** was subjected to ozonolysis and reductive amination with benzylamine followed (**116**). The Boc on the azetidine was transiently removed to relieve steric constraints, so that pyrrolidinone ring was formed by the intramolecular amidation (**117**). After LAH reduction, the nitrogen of the azetidine was re-protected with Boc group and the fully-protected head motif of JTE-052 was obtained in an enantiomerically pure form (**118**). The head group was coupled

with the hinge binder after *N*-benzyl deprotection and the resultant **119** led to JTE-052 by Boc deprotection and subsequent cyanoacetylation (Scheme 11).

Scheme 11. Stereoselective synthesis of JTE-052.[a]

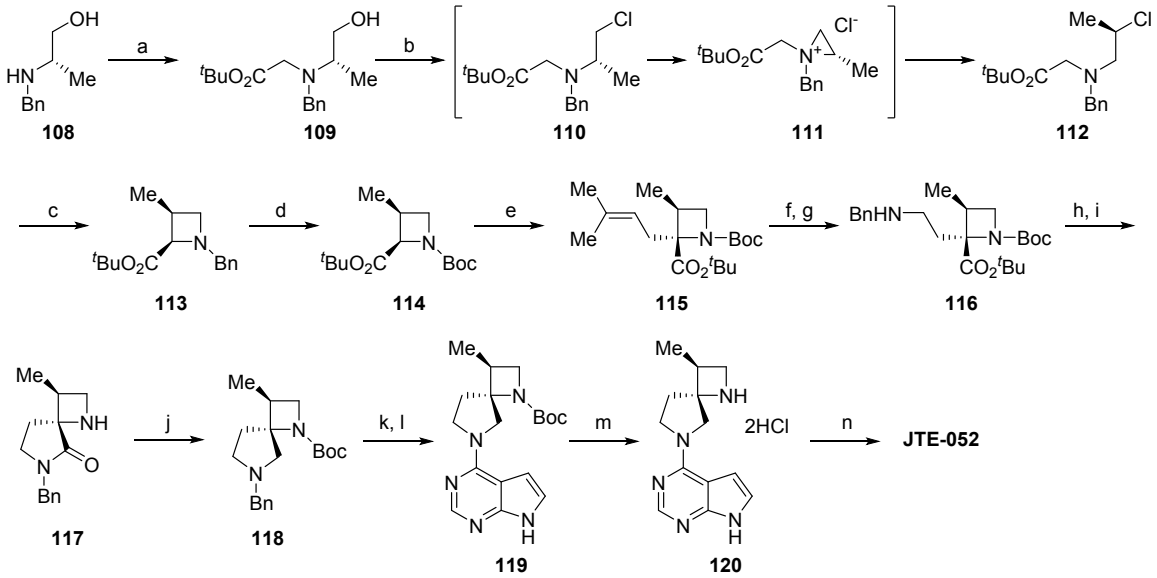

[a]Reagents and conditions:(a) $BrCH_2CO_2t$-Bu, K_2CO_3, DMF, 70 °C; (b) $SOCl_2$, DMF, 60 °C; (c) LiHMDS, HMPA, THF, −78 °C to 0 °C; (d) H_2 (4 atm) $Pd(OH)_2/C$, $(BOC)_2O$, THF, MeOH, rt; (e) $BrCH_2CH{=}CMe_2$, LiHMDS, THF, −78 °C to −20 °C; (f) O_3, PPh_3, $CHCl_3$, MeOH, −78 °C; (g) $BnNH_2$, $NaBH(OAc)_3$, THF, rt; (h) 4 N HCl in 1,4-dioxane, H_2O; (i) HATU, *i*-Pr_2NEt, DMF, rt; (j) $LiAlH_4$, H_2SO_4, THF, 0 °C then $(BOC)_2O$, rt; (k) H_2 (4 atm) $Pd(OH)_2/C$, MeOH, rt; (l)**73**, K_2CO_3, H_2O, 100 °C; (m) 4 N HCl in 1,4-dioxane, $CHCl_3$, MeOH, 60 °C; (n) 3-(3,5-dimethyl-1*H*-pyrazol-1-yl)-3-oxopropanenitrile, *i*-Pr_2NEt, 1,4-dioxane, 100 °C.

CONCLUSIONS

While smaller molecules generally may exhibit better physicochemical properties such as solubility and cell-membrane permeability, they may also potentially bind more targets, which may lead to loss of target specificity. To overcome this potential loss of target specificity, one may wish to consider increasing molecular complexity. Three-dimensionality, which can be characterized by an Fsp^3 value, is one aspect of molecular complexity.[40–42] Upon further review, it is noteworthy that the Fsp^3 values for several JAK inhibitors we synthesized—including compound **47** (0.53) and JTE-052 (0.50)—exceed the benchmark value (0.47)[40] of many marketed drugs.

Among several cytokine signaling pathways in which JAK enzymes are involved, the IL-31 pathway is of particular interest, as transgenic mice in which that pathway is perturbed were previously reported to develop both skin lesions and serological abnormalities,[43] mirroring diagnostic criteria for human AD.[44,45] Additionally, barrier defects in the skin surface are commonly observed in AD patients, which stimulate IL-4 secretion from Th2 cells. Elevated IL-4 production in turn suppresses lipid production and exacerbates barrier disruption.[46] The inhibition of JAK signaling pathways thus may be an effective strategy to treat AD patients and restore barrier function.[47,48] As a matter of fact, topical tofacitinib in 2016 was reported to be effective

for the treatment of AD patients,[49] and the development of JAK inhibitors as anti-AD drugs is currently an active field.[50]

Clinical trials on JTE-052, known as "delgocitinib", for a treatment of atopic dermatitis (AD) have been completed.[51,52] In view of delgocitinib ointment's results in clinical trials, we submitted an New Drug Application (NDA),[53] and have recently received marketing approval for the treatment of atopic dermatitis in Japan.[54]

EXPERIMETAL SECTION

Chemistry. Unless otherwise specified, materials were obtained from commercial suppliers and used without further purification. ^{1}H NMR spectra and ^{13}C NMR spectra were recorded on a JEOL JNM-AL400, Bruker AVANCEIII 400, or Varian MERCURY plus 400 spectrometer in a solution of $CDCl_3$ or DMSO-d_6 using tetramethylsilane as the internal standard. Chemical shifts are expressed as δ (ppm) values for protons relative to the internal standard. Standard abbreviations indicating multiplicity were used as follows: s = singlet, br s = broad singlet, d = doublet, dd = double doublet, dt = double triplet, t = triplet, q = quartet, and m = multiplet. All compounds gave spectra consistent with their assigned structures. HRMS spectra were recorded on an LC-MS

system composed of Agilent 1290 Infinity LC and Thermo Fisher LTQ-Orbitrap Velos. Optical rotation was measured at 20 °C with a Rudolph Research Analytical AUTOPOL V spectrometer. Combustion analyses were performed with a Perkin–Elmer 2400 series II CHNS/O analyzer, and all values were within ±0.4% of the calculated values. Preparative HPLC was performed on a Japan Analytical Industry Co., Ltd. LC-908 instrument. Analytical HPLC was performed on a SHIMADZU Prominence instrument. Single-crystal X-ray analysis was performed with Rigaku R-AXIS RAPID analysis system. Microwave reactions were performed using a Biotage Initiatior eight instrument. The purities of the assayed compounds were determined by analytical HPLC under following conditions [Column: SHIMADZU Shim-pack XR-ODS (3 × 50 mm, 2.2 μm); mobile phase A: 0.1% TFA in water; mobile phase B: 0.1% TFA in CH_3CN; gradient: 10% B to 90% B from 0 to 5 min, 90% B from 5 to 7 min, 90% B to 10% B from 7 to 7.5 min, 10% B from 7.5 to 10 min; flow rate: 8.0 mL/min; detection wavelength: 254 nm] and was ≥ 95%. The detailed synthesis of compounds **3**–**43** are described in the supporting information.

3-(7-(7*H*-Pyrrolo[2,3-*d*]pyrimidin-4-yl)-1,7-diazaspiro[4.5]decan-1-yl)-3-oxopropanenitrile (47). Step 1: A mixture of 4-chloro-7*H*-pyrrolo[2,3-*d*]pyrimidine (94 mg, 0.611 mmol), *t*-butyl 1,7-diazaspiro[4.5]decane-1-carboxylate (176 mg, 0.733 mmol), and K_2CO_3 (253 mg, 1.83 mmol) in H_2O (1 mL) was stirred at 100 ºC overnight.

After cooling to room temperature, the mixture was diluted with EtOAc and H_2O. The resulting mixture was extracted with EtOAc. The organic layer was washed with H_2O and brine, and dried over Na_2SO_4. After filtration and concentration, the residue was purified by flash chromatography (EtOAc:$CHCl_3$ = 1:2 to 2:1 (v/v)) to afford *t*-butyl 7-(7*H*-pyrrolo[2,3-*d*]pyrimidin-4-yl)-1,7-diazaspiro[4.5]decane-1-carboxylate (189 mg, 86% yield). ^{1}H NMR (400 MHz, $CDCl_3$) δ: 10.90–10.58 (m, 1H), 8.30 (br s, 1H), 7.07 (br s, 1H), 6.48–5.65 (m, 1H), 4.87–4.66 (m, 1H), 4.62–4.52 (m, 1H), 3.95–3.82 (m, 0.6H), 3.75–3.50 (m, 1.4H), 3.50–3.31 (m, 1H), 3.20–3.04 (m, 0.6H), 3.04–2.85 (m, 1H), 2.74–2.58 (m, 0.4H), 2.14–1.98 (m, 1H), 1.90–1.40 (m, 6H), 1.54 (s, 3.6H), 1.48 (s, 5.4H).

Step 2: To a solution of this compound obtained previous step (189 mg, 0.528 mmol) in EtOAc (1.0 mL) was added 2 N HCl in MeOH (1.5 mL) and 4 N HCl in EtOAc (3.0 mL) at room temperature. After being stirred at room temperature for 3 h, the mixture was concentrated. The residue was neutralized with 4 N NaOH (0.29 mL) and extracted with $CHCl_3$. The organic layer was washed with H_2O and brine, and dried over Na_2SO_4. After filtration and concentration, the resultant solids were purified by trituration with Et_2O to give 7-(7*H*-pyrrolo[2,3-*d*]pyrimidin-4-yl)-1,7-

diazaspiro[4.5]decane (108 mg, 80% yield). ^{1}H-NMR (400 MHz, $CDCl_3$) δ: 9.26 (br s, 1H), 8.28 (s, 1H), 7.04 (d, *J* = 3.7 Hz, 1H), 6.52 (d, *J* = 3.7 Hz, 1H), 3.92–3.86 (m, 2H), 3.81 (d, *J* = 13.0 Hz, 1H), 3.72 (d, *J* = 13.0 Hz, 1H), 3.10–3.00 (m, 2H), 1.94–1.80 (m, 3H), 1.78–1.70 (m, 5H), 1.55–1.47 (m, 1H).

Step 3: A mixture of this compound obtained previous step (70 mg, 0.272 mmol) and 3-(3,5-dimethyl-1*H*-pyrazol-1-yl)-3-oxopropanenitrile (67 mg, 0.410 mmol) in 1,4-dioxane (1.4 mL) was stirred at 80 °C overnight. After cooling to room temperature and evaporation, the residue was purified by preparative TLC ($CHCl_3$:MeOH = 10 : 1 (v/v)) to give the title compound **47** (104 mg, 86%). ^{1}H NMR (400 MHz, DMSO-d_6) δ: 11.64 (br s, 1H), 8.10 (s, 1H), 7.16 (dd, *J* = 3.4, 2.6 Hz, 1H), 6.57 (dd, *J* = 3.6, 1.6 Hz, 1H), 4.73–4.66 (m, 1H), 4.52 (d, *J* = 12.5 Hz, 1H), 3.93 (s, 2H), 3.83 (d, *J* = 12.9 Hz, 1H), 3.58–3.51 (m, 1H), 3.46–3.39 (m, 1H), 2.99–2.84 (m, 2H), 1.90–1.70 (m, 4H), 1.67–1.57 (m, 2H), 1.56–1.49 (m, 1H). HRMS m/z: $[M+H]^+$ calcd for $C_{17}H_{21}N_6O$, 325.1771; found, 325.1700. Purity: 100%. Chiral resolution of compound **47** to obtained ***ent*-47** as follows. Compound **47** (50 mg) was subjected to nomal phase preparative HPLC under following condition [column: DAICEL CHIRALCEL AD (20 × 250 mm); mobile phase: MeOH] to afford second eluting isomer (***ent*-47**) (16 mg). ^{1}H

NMR (400 MHz, DMSO-d_6) δ: 11.69 (br s, 1H), 8.09 (s, 1H), 7.19–7.15 (m, 1H), 6.59–6.55 (m, 1H), 4.74–4.66 (m, 1H), 4.55–4.47 (m, 1H), 3.95 (s, 2H), 3.86–3.78 (m, 1H), 3.57–3.48 (m, 1H), 3.45–3.37 (m, 1H), 2.99–2.82 (m, 2H), 1.89–1.68 (m, 4H), 1.66–1.56 (m, 2H), 1.55–1.47 (m, 1H). ^{13}C NMR (100 MHz, DMSO-d_6) δ: 162.03, 156.72, 152.35, 151.03, 121.61, 116.46, 101.94, 101.20, 65.82, 49.14, 48.84, 45.45, 35.08, 32.08, 27.85, 23.48, 22.41. HRMS m/z: $[M+H]^+$ calcd for $C_{17}H_{21}N_6O$, 325.1771; found, 325.1766. Purity: 100.0%. $[\alpha]^{20}_D$ +185.58° (c 1.04, MeOH).

The following compounds (**44–46** and **48–49**) were prepared by using the procedures described for the synthesis of **47**. In these cases, corresponding amines were used instead of *t*-butyl 1,7-diazaspiro[4.5]decane-1-carboxylate.

3-(7-(7*H*-Pyrrolo[2,3-*d*]pyrimidin-4-yl)-1,7-diazaspiro[4.4]nonan-1-yl)-3-oxopropanenitrile (44). ^{1}H NMR (400 MHz, DMSO-d_6) δ: 11.59 (br s, 1H), 8.08 (s, 1H), 7.10 (dd, *J* = 3.4, 2.4 Hz, 1H), 6.56–6.52 (m, 1H), 4.36–4.17 (m, 1H), 4.10–3.94 (m, 1H), 3.99 (s, 2H), 3.76–3.19 (m, 4H), 3.05–2.92 (m, 1H), 2.01–1.94 (m, 2H), 1.93–1.83 (m, 2H), 1.81–1.72 (m, 1H). HRMS m/z: $[M+H]^+$ calcd for $C_{16}H_{19}N_6O$, 311.1615; found, 311.1603. Purity: 100%.

3-(2-(7*H*-Pyrrolo[2,3-*d*]pyrimidin-4-yl)-2,6-diazaspiro[4.5]decan-6-yl)-3-oxopropanenitrile (45). ^{1}H NMR (400 MHz, DMSO-d_6) δ: 11.60 (br s, 1H), 8.08 (s, 1H), 7.13–7.10 (m, 1H), 6.57–6.51 (m, 1H), 4.32–4.26 (m, 1H), 4.07 (s, 2H), 4.00–3.50 (m, 3H), 3.48–3.32 (m, 2H), 2.60–2.52 (m, 1H), 2.30–2.08 (m, 1H), 1.82–1.44 (m, 6H). HRMS m/z: $[M+H]^+$ calcd for $C_{17}H_{21}N_6O$, 325.1771; found, 325.1764. Purity: 99.0%.

3-(7-(7*H*-Pyrrolo[2,3-*d*]pyrimidin-4-yl)-2,7-diazaspiro[4.4]nonan-2-yl)-3-oxopropanenitrile (46). ^{1}H NMR (400 MHz, DMSO-d_6) δ: 11.58 (s, 1H), 8.07 (d, J = 2.3 Hz, 1H), 7.12–7.09 (m, 1H), 6.60–6.56 (m, 1H), 3.96–3.89 (m, 2H), 3.88–3.60 (m, 4H), 3.57–3.40 (m, 4H), 2.06–1.84 (m, 4H). HRMS m/z: $[M+H]^+$ calcd for $C_{16}H_{19}N_6O$, 311.1615; found, 311.1607. Purity: 100%.

3-(8-(7*H*-Pyrrolo[2,3-*d*]pyrimidin-4-yl)-1,8-diazaspiro[5.5]undecan-1-yl)-3-oxopropanenitrile (48). ^{1}H NMR (400 MHz, DMSO-d_6) δ: 11.68 (br s, 1H), 8.10 (s, 1H), 7.17 (dd, J = 3.5, 2.6 Hz, 1H), 6.59 (dd, J = 3.7, 1.9 Hz, 1H), 4.64–4.59 (m, 1H), 4.51–4.44 (m, 1H), 4.26–4.21 (m, 1H), 4.07 (d, J = 18.8 Hz, 1H), 4.01 (d, J = 18.6 Hz, 1H), 3.31–3.13 (m, 2H), 2.77–2.67 (m, 1H), 1.86–1.37 (m, 10H). HRMS m/z: $[M+H]^+$ calcd for $C_{18}H_{23}N_6O$, 339.1928; found, 339.1927. Purity: 100%.

3-(2-(7*H*-Pyrrolo[2,3-*d*]pyrimidin-4-yl)-2,7-diazaspiro[5.6]dodecan-7-yl)-3-oxopropanenitrile (49). ^{1}H NMR (400 MHz, DMSO-d_6) δ: 11.63 (br s, 1H), 8.09 (s, 1H), 7.15 (dd, *J* = 3.5, 2.6 Hz, 1H), 6.64 (dd, *J* = 3.6, 2.0 Hz, 1H), 4.53 (d, *J* = 13.2 Hz, 1H), 4.38–4.29 (m, 1H), 4.18 (d, *J* = 13.0 Hz, 1H), 4.02 (s, 2H), 3.35–3.31 (m, 3H), 2.63–2.55 (m, 1H), 1.88–1.77 (m, 2H), 1.74–1.50 (m, 6H), 1.47–1.34 (m, 3H). HRMS m/z: $[M+H]^+$ calcd for $C_{19}H_{25}N_6O$, 353.2084; found, 353.2076. Purity: 100%.

1-(7-(7*H*-Pyrrolo[2,3-*d*]pyrimidin-4-yl)-1,7-diazaspiro[4.5]decan-1-yl)ethan-1-one (50). To a solution of 7-(7*H*-pyrrolo[2,3-*d*]pyrimidin-4-yl)-1,7-diazaspiro[4.5]decane (25 mg, 0.097 mmol) in $CHCl_3$ (1.0mL) was added *i*-Pr_2NEt (0.051 mL, 0.29 mmol) and Ac_2O (0.018 mL, 0.19 mmol) at 0 °C. After being stirred for 1 h at 0 °C, the mixture was diluted with $CHCl_3$ and sat. $NaHCO_3$. The resulting mixture was extracted with $CHCl_3$. The organic layer was washed with brine, dried over Na_2SO_4. After filtration and concentration, the residue was purified by preparative TLC ($CHCl_3$:MeOH = 10:1 (v/v)) to give the title compound **50** (21.8 mg, 75% yield). ^{1}H NMR (400 MHz, DMSO-d_6) δ: 11.65 (br s, 1H), 8.09 (s, 1H), 7.15 (dd, *J* = 3.4, 2.5 Hz, 1H), 6.57 (dd, *J* = 3.6, 1.9 Hz, 1H), 4.73–4.65 (m, 1H), 4.47 (d, *J* = 12.1 Hz, 1H), 3.90 (d, *J* = 12.4 Hz, 1H), 3.62–3.54 (m, 1H), 3.48–3.41 (m, 1H), 3.00–2.88 (m, 2H), 1.97 (s, 3H), 1.88–1.67 (m,

4H), 1.65–1.53 (m, 2H), 1.50–1.43 (m, 1H). HRMS m/z: $[M+H]^+$ calcd for $C_{16}H_{22}N_5O$, 300.1819; found, 300.1817. Purity: 97.4%.

1-(7-(7*H*-Pyrrolo[2,3-*d*]pyrimidin-4-yl)-1,7-diazaspiro[4.5]decan-1-yl)-2-hydroxyethan-1-one (51). Step 1: To a solution of 7-(7*H*-pyrrolo[2,3-*d*]pyrimidin-4-yl)-1,7-diazaspiro[4.5]decane (32 mg, 0.13 mmol) in $CHCl_3$ (0.6 mL) was added Et_3N (0.019 mL, 0.14 mmol) and acetoxyacetyl chloride (0.015 mL, 0.14 mmol) at 0 °C. After being stirred for 1 h at 0 °C, the mixture was diluted with $CHCl_3$ and sat. $NaHCO_3$. The resulting mixture was extracted with $CHCl_3$. The organic layer was washed with brine, dried over Na_2SO_4. After filtration and concentration, the residue was purified by preparative TLC ($CHCl_3$:MeOH = 10:1 (v/v)) to give 2-(7-(7*H*-pyrrolo[2,3-*d*]pyrimidin-4-yl)-1,7-diazaspiro[4.5]decan-1-yl)-2-oxoethyl acetate (17 mg, 38% yield). ^{1}H-NMR (400 MHz, $CDCl_3$) δ: 10.68 (s, 1H), 8.28 (s, 1H), 7.08 (d, *J* = 3.2 Hz, 1H), 6.51 (d, *J* = 3.5 Hz, 1H), 4.72 (d, *J* = 12.8 Hz, 1H), 4.67–4.59 (m, 2H), 4.04 (d, *J* = 12.8 Hz, 1H), 3.58–3.42 (m, 2H), 3.22–3.07 (m, 2H), 2.51–2.31 (m, 1H), 2.22 (s, 3H), 2.15–2.06 (m, 1H), 2.03–1.82 (m, 3H), 1.80–1.55 (m, 3H).

Step 2: A mixture of this compound obtained previous step (15 mg, 0.042 mmol) and K_2CO_3 (17 mg, 0.12 mmol) in MeOH (0.7 mL) was stirred at room temperature

overnight. After the mixture was diluted with EtOAc and H_2O, the mixture was extracted with EtOAc. The organic layer was washed with H_2O and brine. After filtration and concentration, the residue was purified by preparative TLC ($CHCl_3$:MeOH = 10:1 (v/v)) to give the title compound **51** (1.3 mg, 9.8% yield). ^{1}H-NMR (400 MHz, $CDCl_3$) δ: 10.67–10.25 (m, 1H), 8.30 (s, 1H), 7.11–7.07 (m, 1H), 6.52 (d, *J* = 3.2 Hz, 1H), 4.78–4.71 (m, 1H), 4.70–4.64 (m, 1H), 4.09 (d, *J* = 15.3 Hz, 1H), 4.04–3.98 (m, 1H), 4.03 (d, *J* = 15.3 Hz, 1H), 3.67 (br s, 1H), 3.50–3.42 (m, 1H), 3.41–3.32 (m, 1H), 3.26–3.17 (m, 1H), 3.17–3.08 (m, 1H), 2.18–2.10 (m, 1H), 2.04–1.58 (m, 6H). HRMS m/z: $[M+H]^+$ calcd for $C_{16}H_{22}N_5O_2$, 316.1768; found, 316.1575. Purity: 100%.

1-(7-(7*H*-Pyrrolo[2,3-*d*]pyrimidin-4-yl)-1,7-diazaspiro[4.5]decan-1-yl)-2-methoxyethan-1-one (52). To a solution of 7-(7*H*-pyrrolo[2,3-*d*]pyrimidin-4-yl)-1,7-diazaspiro[4.5]decane (50 mg, 0.194 mmol) in $CHCl_3$ (1.0 mL) was added Et_3N (0.030 mL, 0.21 mmol) and 2-methoxyacetyl chloride (0.020 mL, 0.21 mmol) at 0 °C. After being stirred for 1 h at 0 °C, the mixture was diluted with $CHCl_3$ and sat. $NaHCO_3$. The resulting mixture was extracted with $CHCl_3$. The organic layer was washed with brine, and dried over Na_2SO_4. After filtration and concentration, the residue was purified by preparative TLC ($CHCl_3$:MeOH = 10:1 (v/v)) to give the title compound **52** (44 mg, 68%

yield). ^{1}H-NMR (400 MHz, DMSO-d_6) δ: 11.67 (br s, 1H), 8.08 (s, 1H), 7.15 (dd, *J* = 3.5, 2.3 Hz, 1H), 6.56 (dd, *J* = 3.6, 1.7 Hz, 1H), 4.72–4.66 (m, 1H), 4.48 (d, *J* = 12.5 Hz, 1H), 3.98 (d, *J* = 14.6 Hz, 1H), 3.94 (d, *J* = 14.8 Hz, 1H), 3.89 (d, *J* = 13.0 Hz, 1H), 3.53–3.46 (m, 1H), 3.39–3.34 (m, 1H), 3.30 (s, 3H), 2.99–2.89 (m, 2H), 1.85–1.66 (m, 4H), 1.62–1.52 (m, 2H), 1.51–1.45 (m, 1H). HRMS m/z: $[M+H]^+$ calcd for $C_{17}H_{24}N_5O_2$, 330.1911; found, 330.1918. Purity: 99.0%.

***N*-(Cyanomethyl)-7-(7*H*-pyrrolo[2,3-*d*]pyrimidin-4-yl)-1,7-diazaspiro[4.5]decane-1-carboxamide (53).** To a solution of 7-(7*H*-pyrrolo[2,3-*d*]pyrimidin-4-yl)-1,7-diazaspiro[4.5]decane (28 mg, 0.11 mmol) in DMA (0.3 mL) was added *i*-Pr_2NEt (0.028 mL, 0.16 mmol) and 4-nitrophenyl (cyanomethyl)carbamate (31 mg, 0.163 mmol) at 0 °C. After being stirred for 1 h at 0 °C, the mixture was diluted with $CHCl_3$ and sat. $NaHCO_3$. The resulting mixture was extracted with $CHCl_3$. The organic layer was washed with brine, dried over Na_2SO_4. After filtration and concentration, the residue was purified by preparative TLC ($CHCl_3$:MeOH = 10:1 (v/v)) to give the title compound **53** (10 mg, 27% yield). ^{1}H-NMR (400 MHz, DMSO-d_6) δ: 11.68 (br s, 1H), 8.10 (s, 1H), 7.16 (dd, *J* = 3.5, 2.6 Hz, 1H), 6.82 (t, *J* = 5.6 Hz, 1H), 6.59 (dd, *J* = 3.7, 1.9 Hz, 1H), 4.75–4.67 (m, 1H), 4.51–4.45 (m, 1H), 4.03 (d, *J* = 5.8 Hz, 2H), 3.86–3.81 (m, 1H),

3.44–3.37 (m, 1H), 3.32–3.25 (m, 1H), 2.97–2.85 (m, 2H), 1.88–1.69 (m, 4H), 1.66–1.52 (m, 2H), 1.52–1.45 (m, 1H). HRMS m/z: $[M+H]^+$ calcd for $C_{17}H_{22}N_7O$, 340.188; found, 340.1868. Purity: 98.7%.

3-(6-(7*H*-Pyrrolo[2,3-*d*]pyrimidin-4-yl)-1,6-diazaspiro[3.5]nonan-1-yl)-3-oxopropanenitrile (54). **Step 1:** To a suspension of NaH (482 mg, 12.1 mmol) in THF was added triethyl phosphonoacetate (2.39 mL, 12.1 mmol) at 0 ºC. After being stirred for 0.5 h at 0 °C, to the mixture was added 1-boc-3-piperidone (2.0 g, 10.0 mmol). The resulting mixture was stirred for 5 h at room temperature. After the mixture was quenched by addition of H_2O, the mixture was extracted with EtOAc. The organic layer was washed with brine, dried over Na_2SO_4. After filtration and concentration, the residue was purified by flash chromatography (*n*-hexane:EtOAc = 5:1) to give the crude of *t*-butyl-3-(2-ethoxy-2-oxoethylidene)piperidine-1-carboxylate (**93**) (2.71g, 98% yield) as a E/Z mixture. A mixture of this compound obtained previous step (2.71g, 10.1 mmol) and NH_3 in MeOH (27 mL) was stirred at 70 ºC in a sealed tube overnight. After being to cooled to room temperature and removal of solvent in vacuo, the residue was purified by flash chromatography (acetone:$CHCl_3$ = 1:4 to 1:1 (v/v)) to give *t*-butyl 3-amino-3-(2-methoxy-2-oxoethyl)piperidine-1-carboxylate (**94**) (631 mg, 23% yield).

^{1}H NMR (400 MHz, $CDCl_3$) δ: 3.69 (s, 3H), 3.52–3.09 (m, 4H), 2.43 (s, 2H), 1.72–1.47 (m, 6H), 1.45 (s, 9H).

Step 2: A mixture of this compound obtained above (631 mg, 2.32 mmol) and 2 N NaOH (1.74 mL, 3.48 mmol) in MeOH (6.3 mL) was stirred at room temperature overnight. After neutralization by addition of 1 N HCl, the mixture was concentrated in vacuo. After addition of MeOH and CH_3CN, the precipitate was removed by filtration and filtrate was evaporated. The obtained residue was purified by trituration with EtOAc to give the crude of 2-(3-amino-1-(*t*-butoxycarbonyl)piperidin-3-yl)acetic acid (**95**) (613 mg). ^{1}H-NMR (400Mz, DMSO-d_6) δ: 8.51 (br s, 1H), 3.68–2.95 (m, 6H), 2.09 (s, 2H), 1.70–1.52 (m, 3H), 1.52–1.34 (m, 1H), 1.39 (s, 9H).

Step 3: A mixture of this compound obtained previous step (491 mg, 1.90 mmol), tris(2-oxo-3-benzoxazolinnyl phosphine oxide (855 mg, 1.90 mmol), and Et_3N (0.53 mL, 3.81 mmol) in CH_3CN (190 mL) was stirred at 100 °C overnight. After being cooled to room temperature, insoluble materials were removed by filtration and the filtrate was concentrated. The residue was purified by flash chromatography ($CHCl_3$:EtOAc = 75:25 to 66:33 (v/v)) to give *t*-butyl 2-oxo-1,6-diazaspiro[3.5]nonane-6-carboxylate (**96**) (391 mg, 85% yield). ^{1}H NMR (400 MHz, $CDCl_3$) δ: 6.03 (br s, 1H), 3.57 (d, *J* =

13.2 Hz, 1H), 3.47–3.39 (m, 1H), 3.42 (d, *J* = 13.2 Hz, 1H), 3.37–3.28 (m, 1H), 2.78 (d, *J* = 14.8 Hz, 1H), 2.64 (d, *J* = 14.8 Hz, 1H), 1.90–1.75 (m, 2H), 1.68–1.59 (m, 2H), 1.46 (s, 9H).

Step 4: A mixture of this compound obtained previous step (391 mg, 1.63 mmol) and NaH (98 mg, 2.44 mmol) was stirred for 15 min at room temperature, followed by addition of benzyl bromide (0.23 ml, 1.96 mmol). After being stirred for 1 h at room temperature, a reaction mixture was quenched by addition of 10 % citric acid aqueous solution. The resulting mixture was extracted with EtOAc. The organic layer was washed with brine and dried over Na_2SO_4. After filtration and concentration, the residue was purified by flash chromatography (*n*-hexane:EtOAc = 2:1 to 1:1 (v/v)) to give *t*-butyl 1-benzyl-2-oxo-1,6-diazaspiro[3.5]nonane-6-carboxylate (**97**) (362 mg, 67% yield). ^{1}H NMR (400 MHz, $CDCl_3$) δ: 7.39–7.22 (m, 5H), 4.49–4.23 (m, 2H), 4.04–3.61 (m, 2H), 2.96–2.70 (m, 2H), 2.70–2.50 (m, 2H), 1.71–1.52 (m, 4H), 1.44 (s, 9H).

Step 5: To a solution of this compound obtained previous step (361 mg, 1.09 mmol) in EtOAc (0.5 mL) was added 4 N HCl in EtOAc (4 mL). After being stirred for 2 h at room temperature followed by removal of solvent, H_2O was poured in the mixture. To the resulting mixture was added sat. $NaHCO_3$ and extracted with a solution of EtOAc

and MeOH. The organic layer was washed with brine, dried over Na_2SO_4. After filtration, the filtrate was concentrated to give 1-benzyl-1,6-diazaspiro[3.5]nonan-2-one (**98**) (226 mg, 90% yield). ^{1}H NMR (400 MHz, $CDCl_3$) δ: 7.36–7.24 (m, 5H), 4.48 (d, *J* = 15.3 Hz, 1H), 4.26 (d, *J* = 15.3 Hz, 1H), 2.92–2.80 (m, 2H), 2.76–2.68 (m, 2H), 2.63 (dd, *J* = 11.9, 1.0 Hz, 1H), 2.45–2.37 (m, 1H), 1.80–1.38 (m, 5H).

Step 6: To a suspension of $LiAlH_4$ (25 mg, 0.65 mmol) in THF (0.5 mL) was added H_2SO_4 at 0 °C. After being stirred 1 h at 0 °C, to the reaction mixture was added a solution of the compound obtained previous step (50 mg, 0.22 mmol) in THF (0.25 mL). The resulting mixture was stirred for 1.5 h at room temperature followed by addition of H_2O (0.025 mL), 4N NaOH (0.025 mL), and H_2O (0.050 mL). After the insoluble materials was removed by filtration, the filtrate was concentrated to give 1-benzyl-1,6-diazaspiro[3.5]nonane (**99**) (45.2 mg, 96% yield). ^{1}H NMR (400 MHz, $CDCl_3$) δ: 7.34–7.18 (m, 5H), 3.68 (d, *J* = 12.9 Hz, 1H), 3.63 (d, *J* = 12.9 Hz, 1H), 3.26–3.20 (m, 1H), 3.17–3.10 (m, 1H), 3.06–3.01 (m, 1H), 2.91–2.84 (m, 1H), 2.61 (dd, *J* = 11.7, 0.8 Hz, 1H), 2.45–2.37 (m, 1H), 2.07–1.89 (m, 3H), 1.71–1.39 (m, 4H).

Step 7: A mixture of this compound obtained previous step (194 mg, 0.897 mmol), 4-chloro-7*H*-pyrrolo[2,3-*d*]pyrimidine (138 mg, 0.897 mmol), and K_2CO_3 (372 mg, 2.69

mmol) in H_2O (2.0 mL) was stirred at 100 °C overnight. After being cooled to room temperature, the mixture was diluted with EtOAc and H_2O. The resulting mixture was extracted with EtOAc. The organic layer was washed with H_2O and brine, and dried over Na_2SO_4. After filtration and concentration, the residue was purified by flash chromatography ($CHCl_3$:acetone = 3:1 to 2:1 (v/v)) to give 4-(1-benzyl-1,6-diazaspiro[3.5]nonan-6-yl)-7*H*-pyrrolo[2,3-d]pyrimidine (178 mg, 60% yield). ^{1}H NMR (400 MHz, $CDCl_3$) δ: 10.08 (br s, 1H), 8.33 (s, 1H), 7.37–7.19 (m, 5H), 7.09–7.06 (m, 1H), 6.64–6.61 (m, 1H), 4.73 (d, *J* = 12.9 Hz, 1H), 4.54–4.46 (m, 1H), 3.74 (s, 2H), 3.34–3.27 (m, 2H), 3.22–3.14 (m, 1H), 3.13–3.04 (m, 1H), 2.14–1.98 (m, 2H), 1.89-1.63 (m, 4H).

Step 8: A solution of this compound obtained previous step (100 mg, 0.300 mmol) in MeOH (1.0 mL) was treated with 10% $Pd(OH)_2$ on activated carbon (100 mg) and stirred under a hydrogen atmosphere (4 atm) for 2 h at room temperature. After removal of the palladium catalyst by Celite® filtration, the filtrate was concentrated to afford the 4-(1,6-diazaspiro[3.5]nonan-6-yl)-7*H*-pyrrolo[2,3-*d*]pyrimidine (90 mg, quantitative). ^{1}H NMR (400 MHz, $CDCl_3$) δ: 8.19 (s, 1H), 7.02 (d, *J* = 3.6 Hz, 1H), 6.35–

6.30 (m, 1H), 4.60–4.44 (m, 1H), 4.08–3.97 (m, 1H), 3.84–3.74 (m, 1H), 3.74–3.64 (m, 1H), 3.60–3.42 (m, 2H), 2.32–2.13 (m, 3H), 2.10–1.60 (m, 4H).

Step 9: Compound **54** was prepared by coupling of this compound obtained previous step with 3-(3,5-dimethyl-1*H*-pyrazol-1-yl)-3-oxopropanenitrile following the procedure described for the synthesis of the compound **47**. ^{1}H NMR (400 MHz, DMSO-d_6) δ: 11.71 (br s, 1H), 8.13 (s, 1H), 7.20 (dd, *J* = 3.5, 2.4 Hz, 1H), 6.64 (dd, *J* = 3.6, 1.9 Hz, 1H), 4.96 (d, *J* = 12.6 Hz, 1H), 4.67–4.60 (m, 1H), 4.11–4.04 (m, 1H), 4.00–3.93 (m, 1H), 3.70 (s, 2H), 3.53 (d, *J* = 12.6 Hz, 1H), 2.98–2.90 (m, 1H), 2.39–2.31 (m, 1H), 2.01–1.93 (m, 3H), 1.83–1.75 (m, 1H), 1.58–1.46 (m, 1H). HRMS m/z: $[M+H]^+$ calcd for $C_{16}H_{19}N_6O$, 311.1615; found, 311.1616. Purity: 100.0%. Chiral resolution of compound **54** to obtained ***ent*-54** was same procedure described for the synthesis of ***ent*-47** as first eluting isomer. ^{1}H NMR (400 MHz, DMSO-d_6) δ: 11.73 (br s, 1H), 8.13 (s, 1H), 7.22–7.18 (m, 1H), 6.67–6.63 (m, 1H), 4.96 (d, *J* = 12.6 Hz, 1H), 4.68–4.60 (m, 1H), 4.11–4.03 (m, 1H), 4.01–3.93 (m, 1H), 3.71 (s, 2H), 3.53 (d, *J* = 12.6 Hz, 1H), 2.98–2.88 (m, 1H), 2.40–2.30 (m, 1H), 2.03–1.90 (m, 3H), 1.83–1.75 (m, 1H), 1.59–1.45 (m, 1H). ^{13}C NMR (100 MHz, DMSO-d_6) δ: 162.13, 156.77, 152.41, 150.93, 121.83, 116.22, 102.13, 101.26, 67.97, 50.84, 45.57, 45.31, 33.37, 26.42, 23.82, 22.10. HRMS m/z:

$[M+H]^+$ calcd for $C_{16}H_{19}N_6O$, 311.1615; found, 311.1610. Purity: 100.0%. $[\alpha]^{20}_D$ +210.00° (c 1.01, MeOH).

3-(7-Methyl-6-(7*H*-pyrrolo[2,3-*d*]pyrimidin-4-yl)-1,6-diazaspiro[3.5]nonan-1-yl)-3-oxopropanenitrile (55). Step 1: To a mixture of 1-(*t*-butoxycarbonyl)-6-methylpiperidine-3-carboxylic acid (2.80 g, 11.5 mmol) and K_2CO_3 (2.39 g, 17.3 mmol) in DMF (14 mL) was added ally bromide (1.29 mL, 15.0 mmol) at room temperature. After being stirred at room temperature overnight, the mixture was diluted with H_2O and a solution of *n*-hexane and EtOAc (1:1, v/v). The resulting mixture was extracted with EtOAc and the organic layer was washed with H_2O and brine, and dried over $MgSO_4$. After filtration and concentration, the residue was purified by flash chromatography (*n*-hexane:EtOAc = 100:0 to 80:20 (v/v)) to give the 3-allyl 1-(*t*-butyl) 6-methylpiperidine-1,3-dicarboxylate (3.19 g, 98% yield). ^{1}H NMR (400 MHz, $CDCl_3$) δ: 5.98–5.85 (m, 1H), 5.36–5.19 (m, 2H), 4.62–4.57 (m, 2H), 4.48–4.07 (m, 1.8H), 3.10–3.04 (m, 0.2H), 2.97–2.85 (m, 0.8H), 2.62–2.58 (m, 0.2H), 2.47–2.37 (m, 0.8H), 2.08–2.00 (m, 0.2H), 1.95–1.27 (m, 4H), 1.46 (s, 7.2H), 1.45 (s, 1.8H), 1.13 (d, *J* = 6.8 Hz, 3H).

Step 2: To a solution of 1.1 M LiHMDS in THF (11.6 mL, 12.8 mmol) was added dropwise a solution of this compound obtained previous step (1.86 g, 6.56 mmol) in THF (30 mL) at −78 °C. The reaction mixture was warmed to 0 °C and then stirred for 1 h. After the mixture was cooled to −78 °C, to the reaction mixture was added dropwise trimethylsilyl chloride (1.90 mL, 14.8 mmol). The resulting mixture was gradually warmed to −50 °C, and stirred for 2 h. The reaction mixture was quenched by H_2O at 0 °C and the mixture was extracted with *n*-hexane. The aqueous layer was acidified with 2 M H_2SO_4 and extracted with EtOAc. The organic layer was washed with H_2O and brine, and dried over $MgSO_4$. After filtration and concentration, the residue was purified by flash chromatography ($CHCl_3$:MeOH = 99:1 to 90:10 (v/v)) to give 3-allyl-1-(*t*-butoxycarbonyl)-6-methylpiperidine-3-carboxylic acid (1.21 g, 65% yield). ^{1}H NMR (400 MHz, $CDCl_3$) δ: 5.83–5.68 (m, 1H), 5.15–5.06 (m, 2H), 4.44–4.34 (m, 1.4H), 4.01 (d, *J* = 13.9 Hz, 0.6H), 3.07 (d, *J* = 13.9 Hz, 0.7H), 2.67 (d, *J* = 13.9 Hz, 0.3H), 2.49 (dd, *J* = 13.9, 6.7 Hz, 0.7H), 2.37–2.21 (m, 1.3H), 2.11–2.03 (m, 0.3H), 1.98–1.79 (m, 1.7H), 1.73–1.66 (m, 0.6H), 1.54–1.25 (m, 1.4H), 1.46 (s, 6.3H), 1.45 (s, 2.7H), 1.13 (d, *J* = 6.7 Hz, 2.1H), 1.11 (d, *J* = 6.7 Hz, 0.9H).

Step 3: A mixture of this compound obtained previous step (1.20 g, 4.23 mmol) and Et_3N (0.89 mL, 6.35 mmol), and DPPA (1.19 mL, 5.51 mmol) in toluene (12 mL) was stirred for 2 h at 100 °C. After being cooled to room temperature, to the reaction mixture was added benzyl alcohol (1.31 mL, 12.7 mmol) followed by DMAP (104 mg, 0.85 mmol). The resulting mixture was stirred at 100 °C overnight. After concentration, the residue was purified by flash chromatography (*n*-hexane:EtOAc = 100:0 to 70:30 (v/v)) to give the *t*-butyl 5-allyl-5-(((benzyloxy)carbonyl)amino)-2-methylpiperidine-1-carboxylate (1.65 g, 99% yield). ^{1}H NMR (400 MHz, $CDCl_3$) δ: 7.42–7.29 (m, 5H), 5.85–5.70 (m, 1H), 5.19–5.01 (m, 4H), 4.68 (br s, 1H), 4.42–4.33 (m, 0.7H), 4.06–3.94 (m, 1.3H), 3.21 (d, *J* = 12.8 Hz, 0.7H), 2.69 (d, *J* = 14.1 Hz, 0.3H), 2.56 (dd, *J* = 14.1, 6.6 Hz, 0.7H), 2.40–2.27 (m, 0.3H), 2.24–2.07 (m, 1H), 1.87–1.75 (m, 1H), 1.67–1.27 (m, 3H), 1.46 (s, 6.3H), 1.45 (s, 2.7H), 1.19 (d, *J* = 6.4 Hz, 2.1H), 1.11 (d, *J* = 6.8 Hz, 0.9H).

Step 4: A solution of this compound obtained previous step (1.65 g, 4.25 mmol) in $CHCl_3$ (16.5 mL) and MeOH (16.5 mL) was cooled to −78 °C and then bubbled through O_3 gas for 3 h. To the reaction mixture was added $NaBH_4$ (482 mg, 12.7 mmol) at the same temperature and then the mixture was warmed to room temperature for a period

of 2 h. Sat. $NaHCO_3$ was poured into the mixture and the mixture was extracted with EtOAc. The organic layer was washed with brine and dried over $MgSO_4$. After filtration and concentration, the residue was purified by flash chromatography (*n*-hexane:EtOAc = 100:0 to 40:60 (v/v)) to give *t*-butyl 5-(((benzyloxy)carbonyl)amino)-5-(2-hydroxyethyl)-2-methylpiperidine-1-carboxylate (950 mg, 60% yield). ^{1}H NMR (400 MHz, $CDCl_3$) δ: 7.39–7.28 (m, 5H), 5.74 (br s, 1H), 5.05 (s, 2H), 4.40–4.27 (m, 1H), 3.97 (d, *J* = 12.4 Hz, 1H), 3.91–3.75 (m, 2H), 3.38 (d, *J* = 12.4 Hz, 1H), 2.46–2.29 (m, 1H), 2.00–1.38 (m, 6H), 1.45 (s, 9H), 1.21 (d, *J* = 6.7 Hz, 3H).

Step 5: A solution of this compound obtained previous step (285 mg, 0.73 mmol) in THF (4.0 mL) was treated with 10% palladium on activated carbon (60 mg) and stirred under a hydrogen atmosphere (4 atm) for 1 h at room temperature. After removal of the palladium catalyst by Celite® filtration, the filtrate was concentrated to afford the crude of *t*-butyl 5-amino-5-(2-hydroxyethyl)-2-methylpiperidine-1-carboxylate (158 mg, 84% yield). This crude product was dissolved in CH_2Cl_2 (7.0 mL) and cooled to 0 °C. To the mixture was added PPh_3 (357 mg, 1.36 mmol) followed by Et_3N (0.378 mL, 2.71 mmol) and CBr_4 (451 mg, 1.36 mmol). After being stirred for 1.5 h at room temperature, the mixture was diluted with sat. $NaHCO_3$ and EtOAc. The resulting

mixture was extracted with EtOAc. The organic layer was washed with sat. $NaHCO_3$ and brine, and dried over $MgSO_4$. After filtration and concentration, the residue was purified by flash chromatography ($CHCl_3$:MeOH:28% NH_3 aq. = 95:3:2 to 83:15:2 (v/v)) to give *t*-butyl 7-methyl-1,6-diazaspiro[3.5]nonane-6-carboxylate (178 mg, 82% yield). ^{1}H NMR (400 MHz, $CDCl_3$) δ: 4.38–4.28 (m, 1H), 4.17 (d, *J* = 13.2 Hz, 1H), 3.56–3.43 (m, 2H), 2.66 (d, *J* = 13.0 Hz, 1H), 2.17–2.08 (m, 1H), 2.05–1.96 (m, 1H), 1.89–1.82 (m, 1H), 1.74–1.39 (m, 3H), 1.47 (s, 9H), 1.10 (d, *J* = 7.1 Hz, 3H).

Step 6: To a solution of this compound obtained previous step (149 mg, 0.62 mmol) in $CHCl_3$ (1.5 mL) was added *i*-Pr_2NEt (0.14 mL, 0.78 mmol) and CbzCl (0.11 mL, 0.78 mmol) at 0°C. After being stirred for 3.5 h at room temperature, the reaction mixture was concentrated. The residue was purified by flash chromatography (*n*-hexane:EtOAc = 100:0 to 75:25 (v/v)) to give 1-benzyl 6-(*t*-butyl) 7-methyl-1,6-diazaspiro[3.5]nonane-1,6-dicarboxylate (206 mg, 89% yield). ^{1}H NMR (400 MHz, $CDCl_3$) δ: 7.40–7.29 (m, 5H), 5.12 (s, 1.2H), 5.07 (s, 0.8H), 4.45–4.35 (m, 0.6H), 4.28–4.18 (m, 0.4H), 4.12–4.02 (m, 0.4H), 3.97–3.81 (m, 2.6H), 3.55–3.36 (m, 0.4H), 3.34–3.17 (m, 0.6H), 2.58–1.86 (m, 3H), 1.74–1.39 (m, 3H), 1.46 (s, 9H), 1.22–1.13 (m, 1.2H), 1.07–0.98 (m, 1.8H).

Step 7: To a solution of this compound obtained previous step (176 mg, 0.47 mmol) in $CHCl_3$ (1.0 mL) was added 4 N HCl in 1,4-dioxane (1.0 mL) at room temperature. After being stirred for 1 h, the mixture was neutralized with 1 N NaOH and extracted with EtOAc. The organic layer was washed with sat. $NaHCO_3$ and brine, dried over $MgSO_4$, and filtrated. The filtrate was concentrated to give the crude of benzyl 7-methyl-1,6-diazaspiro[3.5]nonane-1-carboxylate. A mixture of this crude product (130 mg, 0.47 mmol), 4-chloro-7*H*-pyrrolo[2,3-*d*]pyrimidine (72 mg, 0.47 mmol), and K_2CO_3 (195 mg, 1.41 mmol) in H_2O (0.72 mL) was heated to 110 °C overnight. The mixture was diluted with $CHCl_3$ and extracted with $CHCl_3$. The organic layer was washed with brine and dried over $MgSO_4$. After filtration and concentration, the residue was purified by flash chromatography (EtOAc:MeOH = 100:0 to 90:10 (v/v)) to give benzyl 7-methyl-6-(7*H*-pyrrolo[2,3-*d*]pyrimidin-4-yl)-1,6-diazaspiro[3.5]nonane-1-carboxylate (99.6 mg, 56% yield). ^{1}H NMR (400 MHz, $CDCl_3$) δ: 10.44–10.38 (m, 1H), 8.31 (s, 1H), 7.41–7.28 (m, 5H), 7.08 (s, 1H), 6.53–6.50 (m, 1H), 5.16 (s, 1.2H), 5.11 (s, 0.8H), 5.03–4.85 (m, 2H), 4.06–3.86 (m, 2H), 3.81–3.74 (m, 0.4H), 3.61–3.51 (m, 0.6H), 2.77–2.65 (m, 0.4H), 2.53–2.41 (m, 0.6H), 2.29–2.16 (m, 1H), 2.00–1.59 (m, 4H), 1.39 (d, *J* = 6.8 Hz, 1.2H), 1.23 (d, *J* = 6.4 Hz, 1.8H).

Step 8: A solution of this compound obtained previous step (99.6 mg, 0.25 mmol) in THF (0.5 mL) and MeOH (0.5 mL) was treated with 10% palladium on activated carbon (50 mg) and stirred under a hydrogen atmosphere (4 atm) for 4 h at room temperature. After removal of the palladium catalyst by Celite® filtration, the filtrate was concentrated to afford 4-(7-methyl-1,6-diazaspiro[3.5]nonan-6-yl)-7*H*-pyrrolo[2,3-d]pyrimidine (62 mg, 96% yield). ^{1}H NMR (400 MHz, DMSO-d_6) δ: 11.65 (br s, 1H), 8.12 (s, 1H), 7.17 (d, *J* = 3.5 Hz, 1H), 6.57 (d, *J* = 3.5 Hz, 1H), 4.97–4.88 (m, 1H), 4.85 (d, *J* = 13.2 Hz, 1H), 3.43–3.26 (m, 2H), 2.87 (d, *J* = 13.0 Hz, 1H), 2.02–1.49 (m, 7H), 1.19 (d, *J* = 6.8 Hz, 3H).

Step 9: Compound **55** was prepared by coupling of this compound obtained previous step with 3-(3,5-dimethyl-1*H*-pyrazol-1-yl)-3-oxopropanenitrile following the procedure described for the synthesis of the compound **47**. The crude product was purified by preparative TLC ($CHCl_3$:MeOH = 85:15 (v/v)) to give the compound **55** (53 mg, 53% yield). ^{1}H NMR (400 MHz, $CDCl_3$) δ: 10.33 (br s, 1H), 8.31 (s, 1H), 7.09 (dd, *J* = 3.5, 2.0 Hz, 1H), 6.53–6.49 (m, 1H), 5.08–4.99 (m, 1H), 4.97–4.88 (m, 1H), 4.29–4.21 (m, 1H), 4.18–4.11 (m, 1H), 3.88–3.81 (m, 1H), 3.25 (s, 2H), 2.88–2.79 (m, 1H), 2.44–2.36 (m, 1H), 2.10–2.02 (m, 1H), 1.92–1.79 (m, 2H), 1.78–1.71 (m, 1H), 1.42 (d,

J = 7.1 Hz, 3H). HRMS m/z: $[M+H]^+$ calcd for $C_{17}H_{21}N_6O$, 325.1771; found, 325.1758. Purity: 98.8%.

The following compounds **56**–**61** were prepared by using the above procedures. In these cases, corresponding carboxylic acid and allyl bromide were used as starting materials.

3-(8-Methyl-6-(7*H*-pyrrolo[2,3-*d*]pyrimidin-4-yl)-1,6-diazaspiro[3.5]nonan-1-yl)-3-oxopropanenitrile (56). Compound **56** was prepared from 1-(*t*-butoxycarbonyl)-5-methylpiperidine-3-carboxylic acid and allyl bromide as starting materials by using the procedure described for the synthesis of the compound **55**. ^{1}H NMR (400 MHz, DMSO-d_6) δ: 11.73 (br s, 1H), 8.12 (s, 1H), 7.22–7.19 (m, 1H), 6.65–6.62 (m, 1H), 4.99–4.92 (m, 1H), 4.64–4.57 (m, 1H), 4.09–4.01 (m, 1H), 4.00–3.92 (m, 1H), 3.69 (s, 2H), 3.49–3.44 (m, 1H), 2.60–2.52 (m, 1H), 2.08–1.90 (m, 4H), 1.75–1.65 (m, 1H), 0.98 (d, *J* = 6.5 Hz, 3H). HRMS m/z: $[M+H]^+$ calcd for $C_{17}H_{21}N_6O$, 325.1771; found, 325.1759. Purity: 100 %.

3-(3-Methyl-6-(7*H*-pyrrolo[2,3-*d*]pyrimidin-4-yl)-1,6-diazaspiro[3.5]nonan-1-yl)-3-oxopropanenitrile (57). Compound **57** was prepared from 1-(*t*-butoxycarbonyl)piperidine-3-carboxylic acid and 3-bromo-2-methyl-1-propene as

starting materials by using the procedure described for the synthesis of the compound **55**. ^{1}H NMR (400 MHz, DMSO-d_6) δ: 11.70 (br s, 1H), 8.14 (s, 1H), 7.18 (dd, *J* = 3.7, 2.6 Hz, 1H), 6.64 (dd, *J* = 3.7, 1.9 Hz, 1H), 5.02–4.96 (m, 1H), 4.65–4.59 (m, 1H), 4.11–4.05 (m, 1H), 3.70 (d, *J* = 18.8 Hz, 1H), 3.65 (d, *J* = 18.8 Hz, 1H), 3.59–3.54 (m, 1H), 3.46–3.42 (m, 1H), 2.97–2.88 (m, 1H), 2.47–2.33 (m, 2H), 2.00–1.93 (m, 1H), 1.87–1.79 (m, 1H), 1.63–1.50 (m, 1H), 0.90 (d, *J* = 7.2 Hz, 3H). HRMS m/z: $[M+H]^+$ calcd for $C_{17}H_{21}N_6O$, 325.1771; found, 325.1760. Purity: 100 %. Chiral resolution of compound **57** to obtained ***ent*-57** was same procedure described for the synthesis of ***ent*-47** as first eluting isomer. ^{1}H NMR (400 MHz, DMSO-d_6) δ: 11.71 (br s, 1H), 8.12 (s, 1H), 7.20 (dd, *J* = 3.5, 2.4 Hz, 1H), 6.65 (dd, *J* = 3.6, 1.9 Hz, 1H), 4.93–4.88 (m, 1H), 4.64–4.58 (m, 1H), 4.24–4.18 (m, 1H), 3.67 (s, 2H), 3.61 (d, *J* = 12.8 Hz, 1H), 3.46–3.41 (m, 1H), 3.03–2.95 (m, 1H), 2.42–2.35 (m, 1H), 2.34–2.25 (m, 1H), 2.15–2.08 (m, 1H), 1.83–1.77 (m, 1H), 1.57–1.43 (m, 1H), 1.01 (d, *J* = 7.1 Hz, 3H). ^{13}C NMR (100 MHz, DMSO-d_6) δ: 162.48, 156.69, 152.39, 150.96, 121.83, 116.21, 102.08, 101.21, 69.12, 53.16, 51.88, 45.35, 32.39, 27.76, 23.98, 23.05, 14.86. HRMS m/z: $[M+H]^+$ calcd for $C_{17}H_{21}N_6O$, 325.1771; found, 325.1759. Purity: 97.5%. $[\alpha]^{20}_{D}$ +168.10° (c 1.05, MeOH).

3-(3,3-Dimethyl-6-(7*H*-pyrrolo[2,3-*d*]pyrimidin-4-yl)-1,6-diazaspiro[3.5]nonan-1-yl)-3-oxopropanenitrile (58). Compound **58** was prepared from 1-(*t*-butoxycarbonyl)piperidine-3-carboxylic acid and 1-bromo-3-methyl-2-butene as starting materials by using the procedure described for the synthesis of the compound **55**. ^{1}H NMR (400 MHz, DMSO-d_6) δ: 11.70 (br s, 1H), 8.15 (s, 1H), 7.19 (dd, *J* = 3.6, 2.5 Hz, 1H), 6.65 (dd, *J* = 3.6, 1.9 Hz, 1H), 5.11–5.03 (m, 1H), 4.60–4.52 (m, 1H), 3.78 (d, *J* = 7.9 Hz, 1H), 3.70 (d, *J* = 18.7 Hz, 1H), 3.65 (d, *J* = 18.7 Hz, 1H), 3.52 (d, *J* = 7.9 Hz, 1H), 3.50–3.46 (m, 1H), 3.07–2.99 (m, 1H), 2.34–2.25 (m, 1H), 2.23–2.18 (m, 1H), 1.91–1.83 (m, 1H), 1.57–1.44 (m, 1H), 1.23 (s, 3H), 0.99 (s, 3H). HRMS m/z: $[M+H]^+$ calcd for $C_{18}H_{24}N_6O$, 339.1928; found, 339.1910. Purity: 100 %.

3-(3,3-Difluoro-6-(7*H*-pyrrolo[2,3-*d*]pyrimidin-4-yl)-1,6-diazaspiro[3.5]nonan-1-yl)-3-oxopropanenitrile (59). Compound **59** was prepared from 1-(*t*-butoxycarbonyl)piperidine-3-carboxylic acid and 3-bromo-3,3-difluoropropene as starting materials by using the procedure described for the synthesis of the compound **55**. ^{1}H NMR (400 MHz, DMSO-d_6) δ: 11.73 (br s, 1H), 8.15 (s, 1H), 7.21 (dd, *J* = 3.4, 2.6 Hz, 1H), 6.64 (dd, *J* = 3.6, 2.0 Hz, 1H), 5.14–5.07 (m, 1H), 4.70–4.46 (m, 3H), 3.83 (d, *J* = 18.9 Hz, 1H), 3.77 (d, *J* = 18.9 Hz, 1H), 3.62–3.56 (m, 1H), 3.00–2.91 (m, 1H),

2.40–2.29 (m, 1H), 2.27–2.20 (m, 1H), 1.99–1.91 (m, 1H), 1.63–1.49 (m, 1H). HRMS m/z: $[M+H]^+$ calcd for $C_{16}H_{17}F_2N_6O$, 347.1426; found, 347.1416. Purity: 99.7 %. Chiral resolution of compound **59** to obtained ***ent*-59** was same procedure described for the synthesis of ***ent*-47** as first eluting isomer. ^{1}H NMR (400 MHz, DMSO-d_6) δ: 11.74 (br s, 1H), 8.15 (s, 1H), 7.22–7.19 (m, 1H), 6.65–6.62 (m, 1H), 5.13–5.07 (m, 1H), 4.69–4.46 (m, 3H), 3.83 (d, J = 18.8 Hz, 1H), 3.77 (d, J = 19.2 Hz, 1H), 3.61–3.55 (m, 1H), 2.99–2.91 (m, 1H), 2.39–2.29 (m, 1H), 2.26–2.19 (m, 1H), 1.99–1.91 (m, 1H), 1.63–1.48 (m, 1H). ^{13}C NMR (100 MHz, DMSO-d_6) δ: 162.48, 156.56, 152.42, 150.71, 122.01, 115.71, 102.82, 101.19, 75.13, 59.25, 45.65, 45.59, 45.02, 27.26, 24.80, 23.14. HRMS m/z: $[M+H]^+$ calcd for $C_{16}H_{17}F_2N_6O$, 347.1426; found, 347.1418. Purity: 100.0%. $[\alpha]^{20}_D$ +139.52° (c 1.04, MeOH).

3-(3-Methyl-6-(7*H*-pyrrolo[2,3-*d*]pyrimidin-4-yl)-1,6-diazaspiro[3.4]octan-1-yl)-3-oxopropanenitrile (60). Compound **60** was prepared from 1-(*t*-butoxycarbonyl)pyrrolidine-3-carboxylic acid and (*E*)-1-bromo-2-butene as starting materials by using the procedure described for the synthesis of the compound **55**. ^{1}H NMR (400 MHz, DMSO-d_6) δ: 11.59 (br s, 1H), 8.07 (s, 1H), 7.11 (dd, J = 3.2, 2.6 Hz, 1H), 6.57 (dd, J = 3.4, 1.7 Hz, 1H), 4.18–4.12 (m, 1H), 4.08–3.92 (m, 3H), 3.84–3.72

(m, 1H), 3.70 (d, *J* = 18.8 Hz, 1H), 3.65 (d, *J* = 18.8 Hz, 1H), 3.59–3.54 (m, 1H), 2.68–2.58 (m, 2H), 2.22–2.11 (m, 1H), 1.11 (d, *J* = 7.2 Hz, 3H). HRMS m/z: $[M+H]^+$ calcd for $C_{16}H_{19}N_6O$, 311.1615; found, 311.1605. Purity: 100 %. Chiral resolution of compound **60** to obtained ***ent*-60** (JTE-052) was same procedure described for the synthesis of ***ent*-47** as second eluting isomer. ^{1}H NMR (400 MHz, DMSO-d_6) δ: 11.60 (br s, 1H), 8.08 (s, 1H), 7.11 (dd, *J* = 3.5, 2.4 Hz, 1H), 6.58 (dd, *J* = 3.4, 1.9 Hz, 1H), 4.18–4.14 (m, 1H), 4.09–3.93 (m, 3H), 3.84–3.73 (m, 1H), 3.71 (d, *J* = 19.0 Hz, 1H), 3.66 (d, *J* = 18.7 Hz, 1H), 3.58 (dd, *J* = 8.2, 6.0 Hz, 1H), 2.70–2.58 (m, 2H), 2.24–2.12 (m, 1H), 1.12 (d, *J* = 7.1 Hz, 3H). ^{13}C NMR (100 MHz, DMSO-d_6) δ: 161.58, 154.43, 151.00, 150.85, 120.51, 115.62, 102.28, 100.61, 73.87, 53.23, 49.92, 46.27, 35.71, 33.00, 23.38, 14.89. HRMS m/z: $[M+H]^+$ calcd for $C_{16}H_{19}N_6O$, 311.1615; found, 311.1606. Purity: 100.0%. $[\alpha]^{20}_D$ +47.09° (c 0.55, MeOH). Anal. ($C_{16}H_{18}N_6O$) calcd C 61.92%, H 5.85%, N 27.08%; found C 61.84%, H, 5.85%, N, 26.86%. Absolutely configuration of ***ent*-60** (JTE-052) was determined by single X-ray crystal structure analysis provided in the Supporting Information.

3-(3,3-Difluoro-6-(7*H*-pyrrolo[2,3-*d*]pyrimidin-4-yl)-1,6-diazaspiro[3.4]octan-1-yl)-3-oxopropanenitrile (61). Compound **61** was prepared from 1-(*t*-

butoxycarbonyl)pyrrolidine-3-carboxylic acid and 3-bromo-3,3-difluoropropene as starting materials by using the procedure described for the synthesis of the compound **55**. ^{1}H NMR (400 MHz, DMSO-d_6) δ: 11.67 (br s, 1H), 8.11 (s, 1H), 7.16 (dd, *J* = 3.3, 2.4 Hz, 1H), 6.58 (dd, *J* = 3.5, 2.0 Hz, 1H), 4.65–4.57 (m, 2H), 4.23–4.14 (m, 2H), 4.12–4.01 (m, 1H), 3.89–3.78 (m, 1H), 3.85 (d, *J* = 19.2 Hz, 1H), 3.79 (d, *J* = 19.0 Hz, 1H), 2.66–2.58 (m, 1H), 2.56–2.46 (m, 1H). HRMS m/z: $[M+H]^+$ calcd for $C_{15}H_{15}F_2N_6O$, 333.1270; found, 333.1250. Purity: 99.4 %. Chiral resolution of compound **61** to obtained ***ent*-61** was the same procedure described for the synthesis of ***ent*-47** using DAICEL CHIRALCEL OD column as first eluting isomer. ^{1}H NMR (400 MHz, DMSO-d_6) δ: 11.68 (br s, 1H), 8.11 (s, 1H), 7.17–7.14 (m, 1H), 6.58 (dd, *J* = 3.3, 1.8 Hz, 1H), 4.66–4.58 (m, 2H), 4.24–4.13 (m, 2H), 4.12–4.02 (m, 1H), 3.89–3.78 (m, 3H), 2.68–2.58 (m, 1H), 2.56–2.45 (m, 1H). ^{13}C NMR (100 MHz, DMSO-d_6) δ: 162.57, 154.85, 151.44, 151.42, 121.53, 115.60, 102.83, 100.85, 80.52, 60.14, 49.45, 49.37, 47.01, 29.03, 24.75. HRMS m/z: $[M+H]^+$ calcd for $C_{15}H_{15}F_2N_6O$, 333.1270; found, 333.1265. Purity: 100.0%. $[\alpha]^{20}_{D}$ +46.67° (c 0.54, MeOH).

Stereoselective synthesis of JTE-052 as described below

Step 1: To a mixture of (*S*)-benzylalaninol (**108**) (111 g, 673 mmol) and K_2CO_3 (111 g, 807 mmol) in DMF (556 mL) was added dropwise *t*-butyl 2-bromoacetate (109 mL, 740 mmol) at 0 °C. After being stirred at room temperature overnight, the mixture was quenched by addition of 6 N HCl (pH = ca. 2). The resulting mixture was extracted with toluene and the organic layer was washed with 0.1 N HCl. The combined aqueous layer was neutralized with 4 N NaOH and extracted with EtOAc. The organic layer was washed with H_2O, sat. $NaHCO_3$, and brine, and then dried over Na_2SO_4. Filtration and concentration in vacuo gave *t*-butyl (*S*)-*N*-benzyl-*N*-(1-hydroxypropan-2-yl)glycinate (**109**) (160.0 g, 89% yield). ^{1}H NMR (400 MHz, $CDCl_3$) δ: 7.40–7.22 (m, 5H), 4.05–3.97 (m, 0.4H), 3.93–3.81 (m, 2H), 3.70–3.65 (m, 0.6H), 3.44–3.38 (m, 0.6H), 3.29 (s, 0.8H), 3.27 (d, *J* = 2.4 Hz, 1.2H), 3.24–3.15 (m, 0.6H), 3.05–2.99 (m, 0.4H), 2.94–2.88 (m, 0.4H), 1.50 (d, *J* = 6.4 Hz, 1.2H), 1.48 (s, 3.6H), 1.45 (s, 5.4H), 1.23 (d, *J* = 6.8 Hz, 1.8H).

Step 2: To a solution of this compound obtained previous step (160 g, 573 mmol) in $CHCl_3$ (640 mL) was added dropwise thionyl chloride (50.0 mL, 687 mmol) at 0 °C and the mixture was stirred at 60 °C for 2 h. After being stirred at 0 °C, the mixture was quenched by addition of sat. $NaHCO_3$ and extracted with $CHCl_3$. The combined

organic layer was dried over Na_2SO_4, filtrated and concentrated in vacuo to give crude of *t*-butyl (*S*)-*N*-benzyl-*N*-(1-chloropropan-2-yl)glycinate (173 g). A solution of the crude of this compound obtained in previous step (173 g) in DMF (520 mL) was stirred at 80 °C for 2.5 h. After being stirred at 0 °C, the mixture was diluted with H_2O and extracted with *n*-hexane/EtOAc (2/1 (v/v)). The combined organic layer was washed with H_2O and brine. After concentration in vacuo, the crude product was purified by flash chromatography (*n*-hexane/EtOAc 50:1 to 40:1 (v/v)) to give *t*-butyl (*R*)-*N*-benzyl-*N*-(2-chloropropyl)glycinate (**112**) (127 g, 75% yield). ^{1}H NMR (400 MHz, $CDCl_3$) δ: 7.37–7.29 (m, 4H), 7.28–7.23 (m, 1H), 4.05–3.97 (m, 1H), 3.91 (d, *J* = 13.5 Hz, 1H), 3.86 (d, *J* = 13.7 Hz, 1H), 3.29 (s, 2H), 3.03 (dd, *J* = 13.9, 6.6 Hz, 1H), 2.91 (dd, *J* = 13.9, 6.8 Hz, 1H), 1.50 (d, *J* = 6.4 Hz, 3H), 1.48 (s, 9H).

Step 3: To a mixture of this compound obtained previous step (60.0g, 202 mmol) and hexamethylphosphoric triamide (36.0 mL) in THF (360 mL) was added dropwise 1.0 M lithium bis(trimethylsilyl)amide in THF (242 mL, 242 mmol) at −78 °C. After the reaction mixture was warmed to 0 °C for the period of 1.5 h, the mixture was quenched by addition of sat. NH_4Cl followed by H_2O at the same temperature. The resulting mixture was extracted with EtOAc. The organic layer was washed with H_2O and brine, and dried over

Na_2SO_4. After filtration and concentration in vacuo, the residue was purified by flash chromatography (*n*-hexane/EtOAc 50/1 to 4/1 (v/v)) to give *t*-butyl (2*R*,3*S*)-1-benzyl-3-methylazetidine-2-carboxylate (**113**) (50.9 g, 97% yield). ^{1}H NMR (400 MHz, $CDCl_3$) δ: 7.34–7.21 (m, 5H), 3.75 (d, *J* = 12.6 Hz, 1H), 3.70–3.67 (m, 1H), 3.58 (d, *J* = 12.6 Hz, 1H), 3.05–3.01 (m, 1H), 2.99–2.95 (m, 1H), 2.70–2.59 (m, 1H), 1.41 (s, 9H), 1.24 (d, *J* = 7.1 Hz, 3H).

Step 4: A mixture of this compound obtained previous step (43.5 g, 167 mmol) and di-*t*-butyl dicarbonate (38.2 g, 175 mmol) in THF (130 mL) and MeOH (130 mL) was treated with 20% palladium hydroxide on activated carbon (3.5 g) and stirred under a hydrogen atmosphere (4 atm) at room temperature for 2 h. After removal of the palladium catalyst by Celite® filtration, the filtrate was concentrated in vacuo to afford di-*t*-butyl (2*R*,3*S*)-3-methylazetidine-1,2-dicarboxylate (**114**) (45.2 g, 99% yield). ^{1}H NMR (400 MHz, DMSO-d_6) δ: 4.44 (d, *J* = 8.8 Hz, 1H), 3.99–3.77 (m, 1H), 3.45–3.37 (m, 1H), 3.00–2.88 (m, 1H), 1.45 (s, 9H), 1.40–1.30 (m, 9H), 1.02 (d, *J* = 7.2 Hz, 3H).

Step 5: To a mixture of this compound obtained previous step (45.2 g, 166 mmol) and 1-bromo-3-methylbut-2-ene (25.4 mL, 216 mmol) in THF (380 mL) was added dropwise 1.0 M lithium bis(trimethylsilyl)amide in THF (200 mL, 200 mmol) at −78 °C. After

the reaction mixture was warmed to −20 °C for the period of 40 min and stirred for 20 min at the same temperature, the mixture was quenched by addition of sat. NH_4Cl followed by H_2O. The resulting mixture was extracted with *n*-hexane/ EtOAc (1/1 (v/v)). The organic layer was washed with H_2O and brine, and dried over $MgSO_4$. After filtration and concentration in vacuo, the residue was purified by flash chromatography (*n*-hexane/EtOAc 15:1 to 8:1 (v/v)) to give di-*t*-butyl (2*R*,3*S*)-3-methyl-2-(3-methylbut-2-en-1-yl)azetidine-1,2-dicarboxylate (**115**) (44.5 g, 79% yield). ^{1}H NMR (400 MHz, $CDCl_3$) δ: 5.29–5.21 (m, 1H), 3.77–3.72 (m, 1H), 3.49–3.44 (m, 1H), 2.73–2.52 (m, 3H), 1.76–1.74 (m, 3H), 1.66–1.65 (m, 3H), 1.51 (s, 9H), 1.43 (s, 9H), 1.05 (d, *J* = 7.3 Hz, 3H).

Step 6: A solution of this compound obtained previous step (44.5 g, 131 mmol) in $CHCl_3$ (310 mL) and MeOH (310 mL) was cooled to −78 °C and then bubbled through O_3 gas for 1 h. The reaction mixture was quenched by addition of a solution of triphenylphosphine (44.7g, 170 mmol) in $CHCl_3$ (45 mL) at −78 °C. After being warmed to room temperature, saturated aqueous solution of $Na_2S_2O_3$ was poured into the mixture. The resulting mixture was extracted with $CHCl_3$. The organic layer was washed with brine and dried over $MgSO_4$. Filtration and concentration in vacuo gave crude of di-*t*-butyl

(2*R*,3*S*)-3-methyl-2-(2-oxoethyl)azetidine-1,2-dicarboxylate (95.0 g). ^{1}H NMR (400 MHz, DMSO-d_6) δ: 9.65 (t, *J* = 2.6 Hz, 1H), 3.79–3.74 (m, 1H), 3.45–3.40 (m, 1H), 2.99–2.80 (m, 3H), 1.46 (s, 9H), 1.34 (s, 9H), 1.06 (d, *J* = 7.2 Hz, 3H).

Step 7: To a solution of this compound obtained previous step (95.0 g) in THF (300 mL) was added benzylamine (34 mL, 328 mmol) at room temperature and the mixture was stirred at same temperature for 2 h. After being cooled to 0 °C, to the mixture was added $NaBH(OAc)_3$ (83.3 g, 393 mmol) and the resulting mixture was stirred at room temperature for 1.5 h. The mixture was diluted with H_2O and extracted with *n*-hexane/EtOAc (1/3 (v/v)). The organic layer was washed with H_2O, brine, and 10 % aqueous solution of citric acid. The combined aqueous layer was neutralized with 4 N NaOH and extracted with $CHCl_3$. The organic layer was washed with brine and dried over $MgSO_4$. After filtration, the filtrate was concentrated in vacuo to give the di-*t*-butyl (2*R*,3*S*)-2-(2-(benzylamino)ethyl)-3-methylazetidine-1,2-dicarboxylate (**116**) (46.6 g, 89% yield from **115**). ^{1}H NMR (400 MHz, DMSO-d_6) δ: 7.34–7.26 (m, 4H), 7.22–7.17 (m, 1H), 3.74–3.65 (m, 2H), 3.61 (t, *J* = 7.8 Hz, 1H), 3.28 (t, *J* = 7.5 Hz, 1H), 2.76–2.66 (m, 2H), 2.57–2.45 (m, 1H), 2.15 (br s, 1H), 2.05–1.89 (m, 2H), 1.42 (s, 9H), 1.27 (s, 9H), 0.96 (d, *J* = 7.1 Hz, 3H).

Step 8: A solution of this compound obtained previous step (46.5 g, 115 mmol) in H_2O (4.1 mL) was added 4 N HCl in 1,4-dioxane (230 mL) at room temperature. After being stirred at 80 °C for 2 h, the mixture was concentrated in vacuo. The crude product was purified by trituration with *n*-hexane/EtOAc (1/1, (v/v)) to give (2*R*,3*S*)-2-(2-(benzylamino)ethyl)-3-methylazetidine-2-carboxylic acid (30.1 g, 82% yield). ^{1}H NMR (400 MHz, DMSO-d_6) δ: 10.24 (br s, 1H), 9.64 (br s, 2H), 8.90 (br s, 1H), 7.58–7.53 (m, 2H), 7.47–7.41 (m, 3H), 4.21–4.10 (m, 2H), 4.02–3.94 (m, 1H), 3.46–3.37 (m, 1H), 3.20–3.10 (m, 1H), 2.99–2.85 (m, 2H), 2.69–2.54 (m, 2H), 1.10 (d, *J* = 7.2 Hz, 3H).

Step 9: To a suspension of this compound obtained previous step (29.1 g, 90.6 mmol) and *i*-Pr_2NEt (65.0 mL, 362 mmol) in $CHCl_3$ (290 mL) was added 1-[bis(dimethylamino)methylene]-1*H*-1,2,3-triazolo[4,5-*b*]pyridinium 3-oxid hexafluorophosphate (41.3 g, 109 mmol) at room temperature. After being stirred at the same temperature, sat. $NaHCO_3$ was poured into the mixture. The resulting mixture was extracted with $CHCl_3$. The organic layer was washed with brine and dried over $MgSO_4$. After filtration and concentration in vacuo, the residue was purified by flash chromatography ($CHCl_3$/MeOH 20:1 to 10:1 (v/v)) to give (3*S*,4*R*)-6-benzyl-3-

methyl-1,6-diazaspiro[3.4]octan-5-one (**117**) (21.3 g, 78% yield). ^{1}H NMR (400 MHz, DMSO-d_6) δ: 7.38–7.31 (m, 2H), 7.30–7.22 (m, 3H), 4.52 (d, *J* = 14.8 Hz, 1H), 4.29 (d, *J* = 14.8 Hz, 1H), 3.35–3.27 (m, 2H), 3.22–3.17 (m, 1H), 3.05 (dd, *J* = 9.5, 4.0 Hz, 2H), 2.77–2.66 (m, 1H), 2.16–2.10 (m, 1H), 1.96–1.87 (m, 1H), 0.94 (d, *J* = 7.1 Hz, 3H).

Step 10: To a suspension of $LiAlH_4$ (6.80 g, 178 mmol) in THF (300 mL) was added dropwise H_2SO_4 (4.8 mL, 88.8 mmol) at 0 °C. After being stirred for 0.5 h, to the mixture was added dropwise a solution of the compound obtained previous step (21.3 g, 74.0 mmol) in THF (100 mL) at same temperature and successively stirred for 1 h. The resulting mixture was quenched by addition of H_2O followed by 4 N NaOH and H_2O. After the reaction mixture was stirred at 0 °C for 0.5 h, the insoluble materials were removed by Celite® filtration. To the resulting filtrate was added $(BOC)_2O$ (19.4 g, 218 mmol) at room temperature. After being stirred for 3 h, the mixture was diluted with sat. NH_4Cl and added *n*-hexane. The organic layer was separated and washed with 10 % aqueous solution of citric acid. The combined aqueous layer was neutralized with 4 N NaOH and extracted with $CHCl_3$. The organic layer was washed with brine and dried over $MgSO_4$. After filtration and concentration, the residue was purified by flash chromatography ($CHCl_3$/MeOH 40:1 to 20:1 (v/v)) to give *t*-butyl (3*S*,4*R*)-6-

benzyl-3-methyl-1,6-diazaspiro[3.4]octane-1-carboxylate (**118**) (15.6 g, 67% yield). ^{1}H NMR (400 MHz, DMSO-d_6) δ: 7.34–7.27 (m, 4H), 7.26–7.21 (m, 1H), 3.84–3.69 (m, 1H), 3.62–3.47 (m, 2H), 3.19–3.05 (m, 1H), 3.02–2.92 (m, 1H), 2.76–2.69 (m, 1H), 2.47–2.24 (m, 4H), 1.95–1.77 (m, 1H), 1.36 (s, 9H), 1.03 (d, J = 7.0 Hz, 3H).

Step 11: A solution of this compound obtained previous step (10.0 g, 31.6 mmol) in THF (50 mL) and MeOH (50 mL) was treated with 20% palladium hydroxide on activated carbon (2.0 g) and stirred under a hydrogen atmosphere (4 atm) at room temperature for 24 h. After removal of the palladium catalyst by Celite® filtration, the filtrate was concentrated in vacuo to afford *t*-butyl (3*S*,4*R*)-3-methyl-1,6-diazaspiro[3.4]octane-1-carboxylate (7.3 g, quantitative). ^{1}H NMR (400 MHz, DMSO-d_6) δ: 3.88–3.71 (m, 1H), 3.44–3.06 (m, 2H), 3.02–2.64 (m, 4H), 2.55–2.38 (m, 1H), 2.31–2.15 (m, 1H), 1.81–1.72 (m, 1H), 1.37 (s, 9H), 1.07 (d, J = 7.0 Hz, 3H).

Step 12: A mixture of this compound obtained previous step (6.9 g, 30.5 mmol), 4-chloro-7*H*-pyrrolo[2,3-*d*]pyrimidine (4.3 g, 27.7 mmol), and K_2CO_3 (7.7 g, 55.4 mmol) in H_2O (65 mL) was stirred at 110 °C for 4 h. After being cooled to room temperature, the mixture was diluted with H_2O. The resulting mixture was extracted with $CHCl_3$/MeOH (1/1 (v/v)). The organic layer was washed with H_2O, sat. NH_4Cl, and

brine, and dried over Na_2SO_4. After filtration and concentration, the residue was purified by flash chromatography ($CHCl_3$/MeOH 50:1 to 20:1 (v/v)) to give *t*-butyl (3*S*,4*R*)-3-methyl-6-(7*H*-pyrrolo[2,3-*d*]pyrimidin-4-yl)-1,6-diazaspiro[3.4]octane-1-carboxylate (**119**) (9.5 g, 99%). ^{1}H NMR (400 MHz, DMSO-d_6) δ: 11.59 (br s, 1H), 8.09 (s, 1H), 7.12–7.09 (m, 1H), 6.64–6.59 (m, 1H), 4.09–3.66 (m, 5H), 3.39–3.21 (m, 1H), 2.64–2.44 (m, 2H), 2.27–2.06 (m, 1H), 1.36 (s, 3H), 1.21 (s, 6H), 1.11 (d, *J* = 6.5 Hz, 3H).

Step 13: To a solution of this compound obtained previous step (9.5 g, 27.7 mmol) in $CHCl_3$ (50 mL) and MeOH (100 mL) was added 4 N HCl in 1,4-dioxane (50 mL) at room temperature. After being stirred at 60 °C for 0.5 h, the mixture was concentrated to afford 4-((3*S*,4*R*)-3-methyl-1,6-diazaspiro[3.4]octan-6-yl)-7*H*-pyrrolo[2,3-*d*]pyrimidine hydrochloride (**120**) (9.3 g, quantitative). ^{1}H NMR (400 MHz, DMSO-d_6) δ: 12.91 (br s, 1H), 9.97–9.64 (m, 2H), 8.45–8.35 (m, 1H), 7.58–7.47 (m, 1H), 7.04–6.92 (m, 1H), 4.99–4.65 (m, 1H), 4.32–3.21 (m, 7H), 3.04–2.90 (m, 1H), 2.46–2.31 (m, 1H), 1.27 (d, *J* = 6.0 Hz, 3H).

Step 14: A mixture of this compound obtained previous step (8.8 g, 27.7 mmol), 3-(3,5-dimethyl-1*H*-pyrazol-1-yl)-3-oxopropanenitrile (6.8g, 41.6 mmol), and *i*-Pr_2NEt

(20.0 mL, 111 mmol) in 1,4-dioxane (100 mL) was stirred at 100 °C for 1 h. After being cooled to room temperature, sat. $NaHCO_3$ was poured into the mixture. The resulting mixture was extracted with $CHCl_3$/MeOH (10/1, (v/v)). The organic layer was washed with brine and dried over Na_2SO_4. After filtration and concentration, the residue was purified by flash chromatography ($CHCl_3$/MeOH 30:1 to 9:1 (v/v)) and successively trituration with *n*-heptane/EtOH (5/1 (v/v)) to give 3-((3*S*,4*R*)-3-methyl-6-(7*H*-pyrrolo[2,3-*d*]pyrimidin-4-yl)-1,6-diazaspiro[3.4]octan-1-yl)-3-oxopropanenitrile (JTE-052) (6.1 g, 71% yield).

Biological assay experimental procedure

Enzyme assay: Recombinant kinases of human JAK1 (850–end) and Tyk2 (871–end) were purchased from Carna Biosciences Inc. (Kobe, Japan), and those of JAK2 (808–end), JAK3 (781–end) and LCK (full-length) were from Millipore Corporation (Bille-rica, MA). HTRF KinEASE – TK kit was from Cisbio Bioassays (Codolet, France). Each enzyme reaction was performed with JAK1, JAK2, JAK3, Tyk2 and LCK enzyme (0.54, 0.004, 0.02, 0.09, and 0.008 μg/mL protein, respectively), 1 μM TK Substrate-Biotin (Cisbio Bioassays), ATP at the Km specific for each enzyme (30, 20, 5, 30 and 30 μM respectively), 5 mM MgCl, 1 mM dithiothreitol, 50 nM Supplement Enzymatic

Buffer (Cisbio Bioassays), and 1 % DMSO in 1x Enzymatic Buffer (Cisbio Bioassays). After the incubation for 60 min at room temperature, enzymatic reaction was stopped by detection reagent containing ethylenediaminetetraacetic acid, Sa-XL665 and TK-Antibody-Cryptate (Cisbio Bioassays) and fluorescence was measured.

Cellular assays: Human peripheral blood was obtained from healthy volunteers with informed consent on the basis of the Declaration of Helsinki. For determination of T cell proliferation induced by IL-2, T cells isolated from human peripheral blood were precultured with 10 µg/mL PHA-M for 3 days and plated in 96-well plates at 1.0 x 10^4 cells/well in the presence of compounds. Following preincubation with the compound for 30 min at 37 °C, the cells were stimulated with 20 ng/mL recombinant human IL-2 and incubated for 3 days at 37 °C. [^{3}H]Thymidine (37 kBq) was added during the culture period. Then the cells were harvested with a 96-well harvester and counted in a scintillation counter. For determination of cytotoxicity, fibroblast proliferation was measured. NHLFs were plated in 96-well plates at 1 x 10^3 cells/well in the presence of compound without the addition of cytokines. The cells were then cultured for 3 days, and [^{3}H]thymidine uptake was measured as described above. For determination of cytokine signaling, human peripheral blood mononuclear cells (hPBMCs; 3 × 10^6

cells/tube) or A549 cells (5×10^5 cells/well) were incubated with a test compound for 30 min at 37°C, and then treated with IL-2 (100 ng/mL), IL-6 (100 ng/mL), IL-23 (100 ng/mL), IFN-α (100 ng/mL), GM-CSF (1 ng/mL), or IL-31 (100 ng/mL) for an additional 15 min. To terminate the stimulation, the cells were fixed with Fixation Buffer (BD Biosciences, San Jose, CA). The fixed cells were incubated with Perm Buffer II (BD Biosciences) on ice and then incubated with fluorochrome-labeled anti-CD3, anti-CD4, or anti-phospho-Stat antibodies for 30 min at room temperature. The cytokine-induced Stat phosphorylation was analyzed and quantified using a Cytomics FC500 (Beckman Coulter Inc., Brea, CA). In the case of IL-23 stimulation, hPBMCs were precultured with 10 μg/mL phytohemagglutinin-M (Sigma-Aldrich Co.) for 3 days to enhance their response to IL-23.

Animals: Lewis rats and BN rats were purchased from Charles River Laboratories Japan, Inc. (Yokohama, Japan). Husbandry conditions were maintained as follows: temperature of 23.0 ± 3.0 °C, humidity of 55 ± 15%, 12 h lighting time (lights on at 8 a.m., lights off at 8 p.m.), CRF-1 pelletized diet (Oriental Yeast Co., Ltd., Tokyo, Japan) supplied ad libitum, and UV-irradiated tap water supplied ad libitum. Animals were treated in accordance with the National Institutes of Health guide for the care and use

of Laboratory animals (NIH Publications No. 8023, revised 1978). Animal study protocols were approved by the Institutional Animal Care and Use Committee of the Central Pharmaceutical Research Institute, Japan Tobacco Inc.

Adjuvant induced arthritis in rat: Lewis rats were injected with 0.1 mL of 5 mg/mL heat-killed *Mycobacterium tuberculosis* H37Ra (Difco Laboratories, Detroit, MI) suspended in liquid paraffin into the base of the tail on day 1 under anesthesia. The compounds were given orally once daily from day 1 to day 28. As an index of paw swelling, the increase in hind paw volume from baseline was measured by a water displacement method using a plethysmometer (Muromachi Kikai Co. Ltd., Tokyo, Japan).

DNCB-induced chronic dermatitis in rat: Thirty micro litter of 0.5% DNCB dissolved in acetone/olive oil (4:1) were applied to ears of BN rats on days 1, 3, 7, 9, 12, 14, 16, 19, and 21. The compounds were administered orally or topically once a day from day 1 to day 21. Ear thickness was measured as an index of ear swelling with a digital thickness gauge (Digimatic Indicator; Mitutoyo Corporation, Kawasaki, Japan) 6 h after DNCB application, and expressed as the increase in thickness from baseline.

ASSOCIATED CONTENT

Supporting Information

The Supporting Information is available free of charge on the ACS Publications website at DOI: 10.1021/acs.jmed-chem.XXXXXXX.

Synthesis for compound **3–43**; HPLC chromatograms of ***ent*-47**, ***ent*-54**, ***ent*-57**, ***ent*-59**, ***ent*-60** (JTE-052), and ***ent*-61**; Chiral HPLC chromatograms of ***ent*-47**, ***ent*-54**, ***ent*-57**, ***ent*-59**, ***ent*-60** (JTE-052), and ***ent*-61**; X-ray crystallographic structure of JAK3 (human) in complex with JTE-052 (PDB code 7C3N); Kinase panel for ***ent*-60** (JTE-052); Single molecule X-ray crystallographic analysis data for ***ent*-60** (JTE-052) (PDF)

Molecular formula strings list (CSV)

AUTHOR INFORMATION

Corresponding Authors.

*e-mail: satoru.noji@jt.com

*e-mail: makoto.shiozaki@jt.com

ORCID

Satoru Noji: 0000-0002-5970-9140

Makoto Shiozaki: 0000-0001-5519-6547

Author Contributions

The manuscript was written through contributions of all authors. All authors have given approval to the final version of the manuscript.

Notes

The authors declare no competing financial interest.

ACKNOWLEDGMENT

We thank Dr. Jun-ichi Haruta and Dr. Hisashi Shinkai for support. We are also grateful to Yasushi Ono, Eita Nagao, and Kenji Fukuda for analytical support.

ABBREVIATIONS

JAK3, Janus kinase 3; SAR, structure–activity relationship; ATP, adenosine 5'-triphosphate; LCK, lymphocyte-specific protein tyrosine kinase; NHLF, normal human lung fibroblasts; IL, interleukin; LE, ligand efficiency; Fsp^3, fraction sp^3; PBMC, peripheral blood mononuclear cell; GM-CSF, granulocyte macrophage colony-stimulating factor; INF-α, interferon-α; ROCK-II, Rho associated coiled-coil containing protein kinase II; AIA, adjuvant-induced arthritis; DNCB, 2,4-dinitrochlorobenzene; AD, atopic dermatitis; DEVEPHOS, 2-(dicyclohexylphosphino)-2'-(dimethylamino)biphenyl; DPEphos, 2,2'-bis(diphenylphosphino)diphenyl ether; WSC·HCl, water soluble carbodiimide hydrochloride, HOBt·H_2O, 1-hydroxy-1H-benzotriazole hydrate; CDI, 1,1'-carbonyldiimidazole; TFAA, trifluoroacetic anhydride; KHMDS, potassium hexamethyldisilazide; LiHMDS, lithium bis(trimethylsilyl)amide; DPPA, diphenylphosphoryl azide; DMAP, *N,N*-dimethyl-4-aminopyridine; HATU, 1-[bis(dimethylamino)methylene]-1*H*-1,2,3-triazolo[4,5-b]pyridinium 3-oxide hexafluorophosphate.

REFERENCES

(1) Eyerich, K.; S. Eyerich, S. Immune response patterns in non-communicable inflammatory skin diseases. *J. Eur. Acad. Dermatol. Venereol.* **2018**, *32*, 692–703.

(2) Lim, H. W.; Collins, S. A. B.; Resneck, J. J. S.; Bolognia, J. L.; Hodge, J. A.; Rohrer, T. A.; Van Beek, M. J.; Margolis, D. J.; Sober, A. J.; Weinstock, M. A.; Nerenz, D. R.; Begolka, W. S.; Moyano, J. V. The burden of skin disease in the United States. *J. Am. Acad. Dermatol.* **2017**, *76*, 958–972.

(3) Noda, S.; Krueger, J. G.; Guttman-Yassky, E. The translational revolution and use of biologics in patients with inflammatory skin diseases. *J. Allergy Clin. Immunol.* **2015**, *135*, 324–336.

(4) Pasparakis, M.; Haase, I.; Nestle, F. O. Mechanisms regulating skin immunity and inflammation. *Nat. Rev. Immunol.* **2014**, *14*, 289–301.

(5) Weidinger, S.; Novak, N. Atopic dermatitis. *Lancet* **2016**, *387*, 1109–1122.

(6) Boehncke W. H.; Schon, M. P. Psoriasis. *Lancet* **2015**, *386*, 983–994.

(7) Bewley, A. Expert consensus: time for a change in the way we advise our patients to use topical corticosteroids. *Br. J. Dermatol.* **2008**, *158*, 917–920.

(8) Ring, J.; Alomar, A.; Bieber, T.; Deleuran, M.; Fink-Wagner, A.; Gelmetti, C.; Gieler, U.; Lipozencic, J.; Luger, T.; Oranje, A. P.; Schafer, T.; Schwennesen, T.;

Seidenari, S.; Simon, D.; Stander, S.; Stingl, G.; Szalai, S.; Szepietowski, J. C.; Taieb A.; Werfel, T.; Wollenberg, A.; Darsow, U.; European Dermatology Forum; European Academy of Dermatology; Venereology; European Task Force on Atopic Dermatitis; European Federation of Allergy; European Society of Pediatric Dermatology; Global Allergy; Asthma European Network. Guidelines for treatment of atopic eczema (atopic dermatitis) part I. *J. Eur. Acad. Dermatol.* **2012**, *26*, 1045–1060.

(9) Menter, A.; Korman, N. J.; Elmets, C. A.; Feldman, S. R.; Gelfand, J. M.; Gordon, K. B.; Gottlieb, A.; Koo, J. Y. M.; Lebwohl, M.; Lim, H. W.; Van Voorhees, A. S.; Beutner, K R.; Bhushan, R. Guidelines of care for the management of psoriasis and psoriatic arthritis section 3. Guidelines of care for the management and treatment of psoriasis with topical therapies *J. Am. Acad. Dermatol.* **2009**, *60*, 643–659.

(10) Paller, A. S.; Kabashima, K.; Bieber, T. Therapeutic pipeline for atopic dermatitis: end of the drought? *J. Allergy Clin. Immunol.* **2017**, *140*, 633–643.

(11) Hengge, U. R.; Ruzicka, T.; Schwartz, R. A.; Cork, M. J. Adverse effects of topical glucocorticosteroids. *J. Am. Acad. Dermatol.* **2006**, *54*, 1–15.

(12) Darnell, J. E. J.; Kerr, I. M.; Stark, G. R.; Jak-STAT pathways and transcriptional activation in response to IFNs and other extracellular signaling proteins. *Science* **1994**, *264*, 1415–1421.

(13) O'Shea J. J.; Gadina, M.; Schreiber, R. D. Cytokine signaling in 2002: new surprises in the Jak/Stat pathway. *Cell* **2002** Apr;109 Suppl:S121–31.

(14) Shuai, K.; Liu, B. Regulation of JAK–STAT singnaling in the immune system. *Nat. Rev. Immunol.* **2003**, *3*, 900–911.

(15) O'Shea, J. J.; Plenge, R. JAK and STAT signaling molecules in immunoregulation and immune-mediated disease. *Immunity* **2012**, *36*, 542–550.

(16) Macchi, P; Villa, A.; Giliani, S.; Sacco, M. G.; Frattini, A.; Porta, F.; Ugazio, A. G.; Johnston, J. A.; Candotti, F.; O'Sheai, J. J.; Vezzoni, P.; Notarangelo, L. D. Mutations of Jak-3 gene in patients with autosomal severe combined immune deficiency (SCID). *Nature* **1995**, *377*, 65–68.

(17) Changelian, P. S.; Flanagan, M. E.; Ball, D. J.; Kent, C. R.; Magnuson, K. S.; Martin, W. H.; Rizzuti, B. J.; Sawyer, P. S.; Perry, B. D.; Brissette, W. H.; McCurdy, S. P.; Kudlacz, E. M.; Conklyn, M. J.; Elliott, E. A.; Koslov, E. R.; Fisher, M. B.; Strelevitz, T. J.; Yoon, K.; Whipple, D. A.; Sun, J.; Munchhof, M. J.; Doty, J. L.;

Casavant, J. M.; Blumenkopf, T. A.; Hines, M.; Brown, M. F.; Lillie, B. M.; Subramanyam, C.; Shang-Poa, C.; Milici, A. J.; Beckius, G. E.; Moyer, J. D.; Su, C.; Woodworth, T. G.; Gaweco, A. S.; Beals, C. R.; Littman, B. H.; Fisher, D. A.; Smith, J. F.; Zagouras, P.; Magna, H. A.; Saltarelli, M. J.; Johnson, K. S.; Nelms, L. F.; Des Etages, S. G.; Hayes, L. S.; Kawabata, T. T.; Finco-Kent, D.; Baker, D. L.; Larson, M.; Si, M. S.; Paniagua, R.; Higgins, J.; Holm, B.; Reitz, B.; Zhou, Y. J.; Morris, R. E.; O'Shea, J. J.; Borie, D. C. Prevention of organ allograft rejection by a specific Janus kinase 3 inhibitor. *Science* **2003**, *302*, 875–878.

(18) Flanagan, M. E.; Blumenkopf, T. A.; Brissette, W. H.; Brown, M. F.; Casavant, J. M.; Shang-Poa, C.; Doty, J. L.; Elliott, E. A.; Fisher, M. B.; Hines, M.; Kent, C.; Kudlacz, E. M.; Lillie, B. M.; Magnuson, K. S.; McCurdy, S. P.; Munchhof, M. J.; Perry, B. D.; Sawyer, P. S.; Strelevitz, T. J.; Subramanyam, C.; Sun, J.; Whipple, D. A.; Changelian, P. S. Discovery of CP-690,550: a potent and selective Janus kinase (JAK) inhibitor for the treatment of autoimmune diseases and organ transplant rejection. *J. Med. Chem.* **2010**, *53*, 8468–8484.

(19) Clark, J. D.; Flanagan, M. E.; Telliez, J.-B. Discovery and development of Janus kinase (JAK) inhibitors for inflammatory diseases. *J. Med. Chem.* **2014**, *57*, 5023–5038.

(20) Schwartz, D. M.; Kanno, Y.; Villarino, A.; Ward, M.; Gadina, M.; O'Shea, J. J. JAK inhibition as a therapeutic strategy for immune and inflammatory diseases. *Nat. Rev. Drug Discovery* **2017**, *16*, 843–862.

(21) Kremer, J. M.; Bloom, B. J.; Breedveld, F. C.; Coombs, J. H.; Fletcher, M, P.; Gruben, D.; Krishnaswami, S.; Burgos-Vargas, R.; Wilkinson, B.; Zerbini, C. A. F.; Zwillich, S. H. The Safety and efficacy of a JAK inhibitor in patients with active rheumatoid arthritis. Results of a double-blind, placebo-controlled phase IIa trial of three dosage levels of CP-690,550 versus placebo. *Arthritis Rheum.* **2009**, *60*, 1895–1905.

(22) Chrencik, J. E.; Patny, A.; Leung, I. K.; Korniski, B.; Emmons, T. L.; Hall, T.; Weinberg, R. A.; Gormley, J. A.; Williams, J. M.; Day, J. E.; Hirsch, J. L.; Kiefer, J. R.; Leone, J. W.; Fischer, H. D.; Sommers, C. D.; Huang, H.-C.; Jacobsen, E. J.; Tenbrink, R. E.; Tomasselli A. G.; Benson, T. E. Structural and thermodynamic

characterization of the TYK2 and JAK3 kinase domains in complex with CP-690550 and CMP-6. *J. Mol. Biol.* **2010**, *400*, 413–433.

(23) Kuntz, I. D.; Chen, K.; Sharp, K. A.; Kollman, P. A. The maximal affinity of ligands. *Proc. Natl. Acad. Sci. U. S. A.* **1999**, *96*, 9997–10002.

(24) Leeson, P. D.; Springthorpe, B. The influence of drug-like concepts on decision-making in medicinal chemistry. *Nat. Rev. Drug Discovery* **2007**, *6*. 881–890.

(25) Abad-Zapatero, C. Ligand efficiency indices for effective drug discovery. *Expert Opin. Drug Discovery* **2007**, *2*, 469–488.

(26) Hopkins, A. L.; Keserü, G. M.; Leeson, P. D.; Rees, D. C.; Charles,s H.; Reynolds, C. H. The role of ligand efficiency metrics in drug discovery. *Nat. Rev. Drug Discovery* **2014**, *13*. 105–121.

(27) Pirrung, M. C.; Liu, Y.; Deng, L.; Halstead, D. K.; Li, Z.; May, J. F.; Wedel, M.; Austin, D. A.; Webster, N. J. G. Methyl Scanning: Total synthesis of demethylasterriquinone B1 and derivatives for identification of sites of interaction with and isolation of its receptor(s). *J. Am. Chem. Soc.* **2005**, *127*, 4609–4624.

(28) These Fsp^3 values were calculated as part of our post analysis of our work on the JAK inhibition project.

(29) Based on the structure of *ent-60* (JTE-052) inferred from the X-ray co-crystal analysis (Figure 2), *ent*-60 (JTE-052) was synthesized according to Scheme 11. The JAK3 inhibitory activity of provided compound accorded with those of *ent*-60. The absolute stereochemistry of *ent*-60 (JTE-052) was afterward confirmed by its X-ray crystallographic analysis. The detailed data was described in Supporting Information.

(30) The detailed kinase panel results are provided in the Supporting Information.

(31) Wang, X.; Magnuson, S.; Pastor, R.; Fan, E.; Hu, H.; Tsui, V.; Deng, W.; Murray, J.; Steffek, M.; Wallweber, H.; Moffat, J.; Drummond, J.; Chan, G.; Harstad, E.; Ebens, A. J. Discovery of novel pyrazolo[1,5-a]pyrimidines as potent pan-Pim inhibitors by structure- and property-based drug design. *Bioorg. Med. Chem. Lett.* **2013**, *23*, 3149–3153.

(32) Thorarensen, A.; Banker, M. E.; Fensome, A.; Telliez, J.-B.: Juba, B.; Vincent, F.; Czerwinski, R. M.; Casimiro-Garcia, A. ATP-mediated kinome selectivity: the missing link in understanding the contribution of individual JAK kinase isoforms to cellular signaling. *ACS Chem. Biol*. **2014**, *9*, 1552–1558.

(33) Vazquez, M. L.; Kaila, N.; Strohbach, J. W.; Trzupek, J. D.; Brown, M. F.; Flanagan, M. E.; Mitton-Fry, M. J.; Johnson, T. A.; TenBrink, R. E.; Arnold, E. P.; Basak, A.; Heasley, S. E.; Kwon, S.; Langille, J.; Parikh, M. D.; Griffin, S. H.; Casavant, J. M.; Duclos,

B. A.; Fenwick, A. E.; Harris, T. M.; Han, S.; Caspers, N.; Dowty, M. E.; Yang, X.; Banker, M. E.; Hegen, M.; Symanowicz, P. T.; Li, L.; Wang, L.; Lin, T. H.; Jussif, J.; Clark, J. D.; Telliez, J.-B.; Robinson, R. P.; Unwalla, R. Identification of N-{cis-3-[methyl(7H-pyrrolo[2,3-d]-pyrimidin-4-yl)amino]cyclobutyl}propane-1-sulfonamide (PF-04965842): a selective JAK1 clinical candidate for the treatment of autoimmune diseases. *J. Med. Chem.* **2018**, *61*, 1130−1152.

(34) Hegen, M.; Keith Jr, J. C.; Collins, M.; Nickerson-Nutter, C. L. Utility of animal models for identification of potential therapeutics for rheumatoid arthritis. *Ann. Rheum. Dis.* 2008, *67*, 1505−1515.

(35) Tanimoto, A.; Shinozaki, Y.; Nozawa, K.; Kimoto, Y.; Amano, W.; Matsuo, A.; Yamaguchi, T.; Matsushita, M. Improvement of spontaneous locomotor activity with JAK inhibition by JTE-052 in rat adjuvant-induced arthritis. *BMC Musculoskelet Disord.* 2015, *16*, 339.

(36) Fujii, Y.; Takeuchi, H.; Sakuma, S.; Sengoku, T.; Takakura, S. Characterization of a 2,4-dinitrochlorobenzene-induced chronic dermatitis model in rats. *Skin Pharmacol. Physiol.* 2009, *22*, 240–247.

(37) Tanimoto, A.; Shinozaki, Y.; Yamamoto, Y.; Katsuda, Y.; Taniai-Riya, E.; Toyoda, K.; Kakimoto, K.; Kimoto, Y.; Amano, W.; Konishi, N.; Hayashi, M. A novel JAK inhibitor JTE-052 reduces skin inflammation and ameliorates chronic

dermatitis in rodent models: comparison with conventional therapeutic agents. *Exp Dermatol*. **2018**, *27*, 22–29.

(38) Nishikawa, T.; Kajii, S.; Isobe, M. Synthesis of model compound containing an indole spiro-β-lactam moiety with vinylchloride in chartellines. *Chem. Lett.* **2004**, *33*, 440–441.

(39) Sivaprakasam, M.; Couty, F.; Evano, G.; Srinivas, B.; Sridhar, R.; Rao, R. Stereocontrolled synthesis of 3-substituted azetidinic amino acids. *Synlett* **2006**, *5*, 781–785.

(40) Lovering, F.; Bikker, J.; Humblet, C. Escape from flatland: increasing saturation as an approach to improving clinical success. *J. Med. Chem.* **2009**, *52*, 6752–6756.

(41) Lovering, F. Escape from flatland 2: complexity and promiscuity. *MedChemComm* **2013**, *4*, 515–519.

(42) Méndez-Lucio, O.; Medina-Franco, J. L. The many roles of molecular complexity in drug discovery. *Drug Discovery Today* **2017**, *22*, 120–126.

(43) Dillon, S. R.; Sprecher, C.; Hammond, A.; Bilsborough, J.; Rosenfeld-Franklin, M.; Presnell, S. R.; Haugen, H. S.; Maurer, M.; Harder, B.; Johnston, J.; Bort, S.; Mudri, S.; Kuijper, J. L.; Bukowski, T.; Shea, P.; Dong, D. L.; Dasovich, M.; Grant,

F. J.; Lockwood, L.; Levin, S. D.; LeCiel, C.; Waggie, K.; Day, H.; Topouzis, S.; Kramer, J.; Kuestner, R.; Chen, Z.; Foster, D.; Parrish-Novak, J.; Gross, J. A. Interleukin 31, a cytokine produced by activated T cells, induces dermatitis in mice. *Nat. Immunol.* **2004**, *5*, 752–760.

(44) Cornelissen, C.; Lüscher-Firzlaff, J.; Baron, J. M.; Lüscher, B.; Signaling by IL-31 and functional consequences. *Eur. J. Cell Biol.* **2012**, *91*, 552–566.

(45) Bao, L.; Zhang, H.; Chan, L. S. The involvement of the JAK-STAT signaling pathway in chronic inflammatory skin disease atopic dermatitis. *JAKSTAT*. **2013** Jul 1;2(3):e24137.

(46) Danso, M. O.; Van Drongelen, V.; Mulder, A.; Van Esch, J.; Scott, H.; Van Smeden, J.; Ghalbzouri, A. El.; Bouwstra, J. A. TNF-α and Th2 cytokines induce atopic dermatitis like features on epidermal differentiation proteins and stratum corneum lipids in human skin equivalents. *J. Invest. Dermatol.* **2014**, *134*, 1941–1950.

(47) Amano, W.; Nakajima, S.; Kunugi, H.; Numata, Y.; Kitoh, A.; Egawa, G.; Dainichi, T.; Honda, T.; Otsuka, A.; Kimoto, Y.; Yamamoto, Y.; Tanimoto, A.; Matsushita, M.; Miyachi, Y.; Kabashima, K. The Janus kinase inhibitor JTE-052

improves skin barrier function through suppressing signal transducer and activator of transcription 3 signaling. *J. Allergy Clin. Immunol.* **2015**, *136*, 667–677.

(48) Yamamoto, Y.; Otsuka, A.; Nakashima, C.; Ishida, Y.; Honda, T.; Egawa, G.; Amano, W.; Usui, K.; Hamada, Y.; Wada, M.; Tanimoto, A.; Konishi, N.; Hayashi, M.; Matsushita, M; Kabashima, K. Janus kinase inhibitor delgocitinib suppresses pruritus and nerve elongation in an atopic dermatitis murine model. *J. Dermatol. Sci.* **2020**, *97*, 161–164.

(49) Bissonnette, R.; Papp, K. A.; Poulin, Y.; Gooderham, M.; Raman, M.; Mallbris, L.; Wang, C.; Purohit, V.; Mamolo, C.; Papacharalambous, J.; Ports, W. C. Topical tofacitinib for atopic dermatitis: a phase IIa randomized trial. *Br. J. Dermatol.* **2016**, *175*, 902–911.

(50) He, H.; Guttman-Yassky, E. JAK inhibitors for atopic dermatitis: an update. *Am. J. Clin. Dermatol.* **2019**, *20*, 181–192.

(51) Nakagawa, H.; Nemoto, O.; Igarashi, A.; Saeki, H.; Kaino, H.; Nagata, T. Delgocitinib ointment, a topical Janus kinase inhibitor, in adult patients with moderate to severe atopic dermatitis: a phase 3, randomized, double-blind,

vehicle-controlled study and an open-label, long-term extension study. *J. Am. Acad. Dermatol.* **2020**, *82*, 823–831.

(52) Nakagawa, H.; Nemoto, O.; Igarashi, A.; Saeki, H.; Murata R.; Kaino, H.; Nagata, T. Long-term safety and efficacy of delgocitinib ointment, a topical Janus kinase inhibitor, in adult patients with atopic dermatitis. *J. Dermatol.* **2020**, *47*, 114–120.

(53) https://www.jt.com/media/news/2019/pdf/20190131_E01.pdf. (accessed Jan, 20, 2020)

(54) https://www.jt.com/media/news/2020/pdf/20200123_E01.pdf (accessed Jan, 28, 2020)

Table of Contents Graphics